Dyson, *ibid.* 4, 701, 713 (1963).
[8]H. Liou, H. S. Camarda, and F. Rahn, Phys. Rev. C 5, 1002 (1972).
[9]J. E. Monahan and N. Rosenzweig, Phys. Rev. C 1, 1714 (1970).
[10]O. Bohigas and J. Flores, in *Proceedings of the International Conference on Statistical Properties of Nuclei, Albany, New York, August 23–27, 1971* (Plenum, New York, 1972), p. 195.
[11]F. Rahn, H. Camarda, G. Hacken, W. W. Havens, Jr., H. I. Liou, J. Rainwater, M. Slagowitz, and S. Wynchank, to be published.
[12]C. M. Newstead, J. Delaroche, and B. Cauvin, in *Proceedings of the International Conference on Statistical Properties of Nuclei, Albany, New York, August 23–27, 1971* (see Ref. 10), p. 367.
[13]K. Seth, Nucl. Data A2, 299 (1966).

PHYSICAL REVIEW C VOLUME 6, NUMBER 1 JULY 1972

# Nuclear Levels in $^{233}$Th Excited by Neutron Capture and $(d, p)$ Reactions*

T. von Egidy, O. W. B. Schult, and D. Rabenstein
*Physik-Department, Technische Universität München, München, Germany*

and

J. R. Erskine
*Argonne National Laboratory, Argonne, Illinois 60439*

and

O. A. Wasson and R. E. Chrien
*Brookhaven National Laboratory, Upton, New York 11973*

and

D. Breitig, R. P. Sharma,† H. A. Baader, and H. R. Koch‡
*Physik-Department, Technische Universität München, München, Germany, and Research Establishment Risö, Risö, Denmark*
(Received 29 February 1972)

Low-energy $\gamma$ rays of the reaction $^{232}$Th$(n,\gamma)^{233}$Th have been measured with the Risö bent-crystal spectrometer and with a Ge(Li) spectrometer at Munich. High-energy neutron-capture $\gamma$ rays from four low-energy neutron resonances have been investigated at the fast-chopper facility at Brookhaven. Data on the reaction $^{232}$Th$(d,p)^{233}$Th were taken with an Enge split-pole magnetic spectrograph at the tandem Van de Graaff accelerator at Argonne. The combination of these data resulted in a level scheme of $^{233}$Th. Seven Nilsson configurations have been assigned to rotational bands, two of them tentatively. Spectroscopic factors have been calculated with $\epsilon_4$ deformation and Coriolis mixing, and compared with the experiment. The neutron binding energy in $^{233}$Th has been determined to be 4786.5± 2.0 keV.

## 1. INTRODUCTION

The deformed nucleus $^{233}$Th is supposed to have a structure similar to its isotone $^{235}$U. The best ways of investigating $^{233}$Th are by means of the $(d,p)$ and $(n,\gamma)$ reactions. Because of the rather small neutron capture cross section of $^{232}$Th (7.4 b), previous $(n,\gamma)$ experiments[1-6] did not result in a level scheme of $^{233}$Th. The $(d,p)$ reaction has recently been measured at Risö.[7]

To obtain more information on $^{233}$Th, experiments have been carried out at Risö, Denmark, through the study of low-energy neutron-capture $\gamma$ rays with a crystal spectrometer, at Munich with a Ge(Li) spectrometer for low-energy capture $\gamma$ rays, at Brookhaven National Laboratory (BNL), where high-energy $\gamma$ rays from resonant neutron capture have been investigated, and at Argonne with the $(d,p)$ reaction. Preliminary results have been reported already.[8,9]

An attempt was made to measure conversion electrons following neutron capture with the $\beta$ spectrometer at the Munich FRM reactor[10] and with the superconducting $\beta$ spectrometer SULEIKA at the Munich FRM reactor.[11] Because of the low capture cross section, only conversion-electron lines with an intensity of more than about 5 per 100 captures should have been observed. No $^{233}$Th lines were found in the conversion-electron spectra.

The knowledge of the level scheme of $^{233}$Th is interesting, since this knowledge is another important ingredient for systematic comparisons of the nuclear structure of the actinides. Insight into nuclear models, in particular the Nilsson model, is gained by these comparisons.

## 2. EXPERIMENTS

### A. Measurement with the Crystal Spectrometer at Risö

The $\gamma$ spectrum between 87 and 900 keV from slow-neutron capture in $^{232}$Th has been measured with the Risö curved-crystal spectrometer.[12] The lines emitted from a 132-mg thorium oxide source were recorded automatically in different orders of reflections with a resolution of

$$\Delta E_\gamma / E_\gamma \approx \frac{0.013E(\mathrm{MeV})}{n},$$

where $\Delta E_\gamma$ is the full width at half maximum (FWHM) of a $\gamma$ line obtained in the $n$th order of reflection. The value of $n$ is 1 for $E_\gamma < 174$ keV, 1 and 2 for $E_\gamma < 261$ keV, 1, 2, and 3 for $E_\gamma < 435$ keV, and 5 for intense transitions with $E_\gamma > 435$ keV. Two sections of the $\gamma$ spectrum are shown in the upper part of Fig. 1. Most of the observed reflections correspond to $\gamma$ transitions in $^{233}$Th. These are listed in Table I. Their energies are based on the value $511.006 \pm 0.002$ keV of the annihilation line[13] and the $K\alpha_1$ and $K\alpha_2$ line energies.[14] The intensities in Table I are calibrated to $\gamma$ rays per 100 captures by using the 311-keV decay line of $^{233}$Pa for which Albridge *et al.*[15] give an absolute intensity of 34% per decay. The calibration error of 15% is not included in the intensity error in the table.

$\gamma$ transitions within $^{233}$U have been measured simultaneously with the $(n, \gamma)$ transitions in $^{233}$Th. The energies of these $\gamma$ rays have been given elsewhere.[16] Some $\gamma$ lines from the $\beta$ decay of $^{233}$Th to $^{233}$Pa have been observed (in keV): $194.90 \pm 0.05$; $440.96 \pm 0.07$; $447.77 \pm 0.3$; $459.26 \pm 0.06$; $499.20 \pm 0.3$; $669.64 \pm 0.2$.

### B. Low-Energy Ge(Li) Detector Measurements at Munich

The $\gamma$ spectrum resulting from neutron capture in $^{232}$Th has been measured between 50 keV and 2.25 MeV with a 30-cm$^3$ coaxial Ge(Li) detector. At 1.33 MeV, this detector yields a linewidth (FWHM) of 2.5 keV and a peak-to-Compton ratio of 19. The target consisted of 9.8 g natural thorium, in the form of a disk with an average thick-

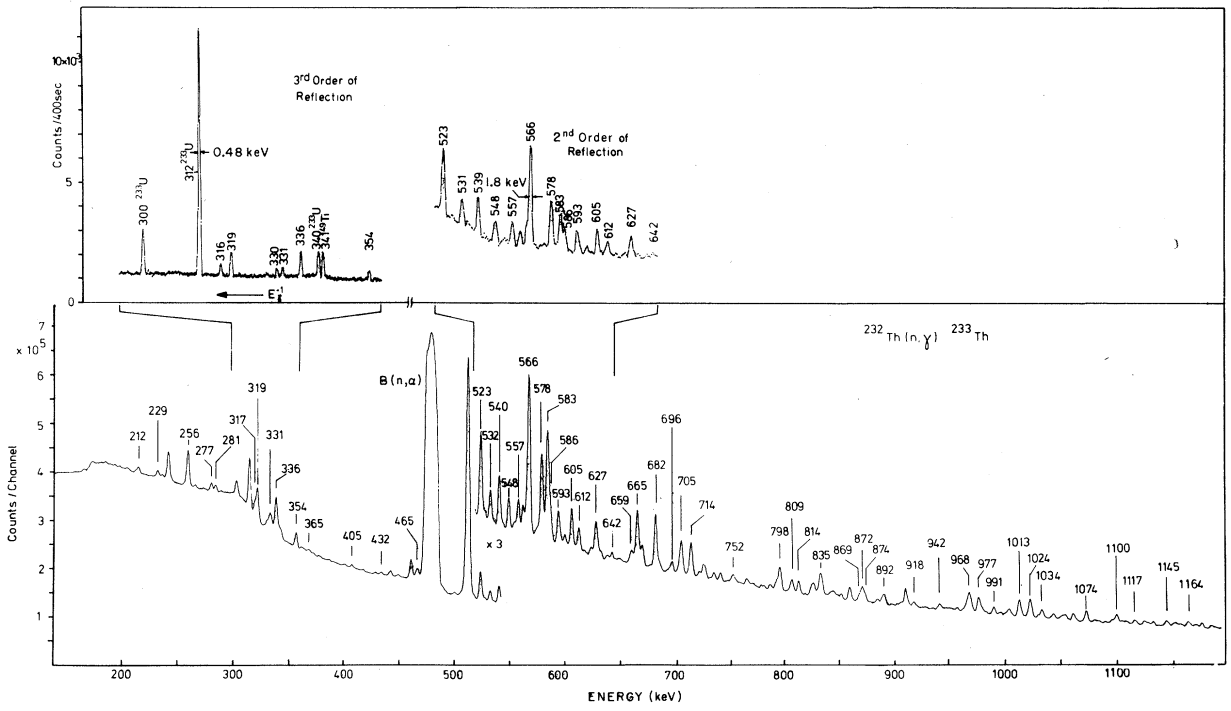


FIG. 1. Lower part: $\gamma$ spectrum from slow-neutron capture measured with the Ge(Li) detector at Munich. Upper part: two sections of the $(n, \gamma)$ spectrum measured with the Risö crystal spectrometer. There is contamination from other reactions in both spectra.

TABLE I. Low-energy capture γ transitions in $^{233}$Th.

| | Crystal spectrometer | | | | Ge(Li) spectrometer | | | |
|---|---|---|---|---|---|---|---|---|
| No. | $E$(keV) [a] | $\Delta E$ | $I/100n$ | $\Delta I$ | $E$(keV) [a] | $\Delta E$ | $I/100n$ | $\Delta I$ |
| 1 | 159.22 | 0.05 | 0.35 | 0.1 | | | | |
| 2 | 182.40? | 0.10 | 0.08 | 0.06 | 181.89? | 0.22 | 0.07 | 0.02 |
| 3 | 201.62 | 0.05 | 0.11 | 0.03 | 201.64 | 0.20 | 0.11 | 0.02 |
| 4 | 211.86 | 0.05 | 0.26 | 0.05 | 211.71 | 0.16 | 0.30 | 0.04 |
| 5 | 229.04 | 0.03 | 0.20 | 0.05 | 229.02 | 0.15 | 0.37 | 0.07 |
| 6 | 233.28 | 0.03 | 0.11 | 0.03 | 232.90 | 0.18 | 0.21 | 0.06 |
| 7 | 256.16 | 0.04 | 1.40 | 0.16 | 256.09 | 0.14 | 1.59 | 0.15 |
| 8 | 260.22? | 0.08 | 0.05 | 0.02 | | | | |
| 9 | 263.02 | 0.08 | 0.10 | 0.02 | 262.60 | 0.18 | 0.12 | 0.02 |
| 10 | 267.71? | 0.20 | 0.04 | 0.02 | | | | |
| 11 | 269.69? | 0.09 | 0.03 | 0.02 | | | | |
| 12 | 277.53 | 0.03 | 0.23 | 0.05 | 277.3 | 0.3 | 0.33 | 0.04 |
| 13 | 278.19 | 0.04 | 0.15 | 0.02 | | | | |
| 14 | 281.32 | 0.02 | 0.20 | 0.03 | 281.16 | 0.15 | 0.26 | 0.04 |
| 15 | 286.4? | | 0.01 | 0.01 | 286.18? | 0.31 | 0.05 | 0.02 |
| 16 | 297.00? | 0.10 | 0.07 | 0.02 | 297.2 | 0.7 | 0.03 | 0.02 |
| 17 | 298.81? | 0.15 | 0.06 | 0.02 | | | | |
| 18 | 316.68 | 0.04 | 0.58 | 0.06 | 316.64 | 0.15 | 0.51 | 0.07 |
| 19 | 319.09 | 0.04 | 1.21 | 0.13 | 318.97 | 0.15 | 1.15 | 0.11 |
| 20 | 327.50 | 0.10 | 0.15 | 0.03 | 328.19+ | 0.22 | 0.43 | 0.05 |
| 21 | 329.93 | 0.03 | 0.34 | 0.04 | | | | |
| 22 | 331.35 | 0.03 | 0.47 | 0.05 | 331.00 | 0.17 | 0.81 | 0.11 |
| 23 | 335.93 | 0.02 | 1.46 | 0.16 | 335.72 | 0.15 | 1.74 | 0.15 |
| 24 | 346.01? | 0.25 | 0.03 | 0.02 | | | | |
| 25 | 351.73? | 0.10 | 0.06 | 0.02 | | | | |
| 26 | 354.32 | 0.03 | 0.57 | 0.06 | 354.09 | 0.15 | 0.63 | 0.03 |
| 27 | 361.9? | 0.3 | 0.06 | 0.02 | 361.74 | 0.21 | 0.10 | 0.02 |
| 28 | 364.98 | 0.15 | 0.10 | 0.03 | 365.02 | 0.23 | 0.13 | 0.02 |
| 29 | 366.7 | 0.3 | 0.07 | 0.02 | 366.89 | 0.25 | 0.12 | 0.02 |
| 30 | 370.46 | 0.07 | 0.10 | 0.03 | 370.18 | 0.18 | 0.10 | 0.02 |
| 31 | 385.22? | 0.15 | 0.08 | 0.03 | 384.30 | 0.25 | 0.06 | 0.02 |
| 32 | | | | | 389.13? | 0.53 | 0.02 | 0.01 |
| 33 | 402.53 | 0.20 | 0.06 | 0.01 | | | | |
| 34 | 405.53 | 0.05 | 0.12 | 0.02 | 405.40 | 0.16 | 0.15 | 0.02 |
| 35 | 427.9 | 0.3 | 0.08 | 0.03 | 426.89 | 0.23 | 0.06 | 0.01 |
| 36 | 432.22 | 0.12 | 0.13 | 0.04 | 431.92 | 0.18 | 0.11 | 0.01 |
| 37 | 465.12 | 0.06 | 0.37 | 0.06 | 464.56? | 0.16 | 0.41 | 0.04 |
| 38 | 472.30 | 0.03 | 2.79 | 0.32 | | | | |
| 39 | 488.00 | 0.12 | 0.17 | 0.05 | | | | |
| 40 | 522.63 | 0.09 | 1.59 | 0.16 | 522.44 | 0.15 | 1.74 | 0.11 |
| 41 | 531.47 | 0.06 | 0.59 | 0.08 | 531.31 | 0.15 | 0.65 | 0.04 |
| 42 | 534.9 | 0.3 | 0.11 | 0.04 | | | | |
| 43 | 539.54 | 0.10 | 0.95 | 0.10 | 539.35 | 0.15 | 1.03 | 0.07 |
| 44 | 543.4 | 0.3 | 0.10 | 0.04 | 542.46 | 0.32 | 0.10 | 0.03 |
| 45 | 548.29 | 0.08 | 0.58 | 0.08 | 547.96 | 0.16 | 0.75 | 0.04 |
| 46 | 553.0 | 0.3 | 0.16 | 0.05 | 553.05 | 0.17 | 0.22 | 0.02 |
| 47 | 556.97 | 0.08 | 0.54 | 0.10 | 556.64 | 0.16 | 0.76 | 0.04 |
| 48 | 561.11 | 0.09 | 0.51 | 0.13 | 560.93+ | 0.16 | 0.65 | 0.04 |
| 49 | 564.57 | 0.09 | 0.53 | 0.08 | 564.12 | 0.17 | 0.65 | 0.05 |
| 50 | 566.68 | 0.06 | 2.95 | 0.44 | 566.36 | 0.15 | 3.70 | 0.22 |

TABLE I *(Continued)*

| No. | Crystal spectrometer | | | | Ge(Li) spectrometer | | | |
|---|---|---|---|---|---|---|---|---|
| | $E$(keV) [a] | $\Delta E$ | $I/100n$ | $\Delta I$ | $E$(keV) [a] | $\Delta E$ | $I/100n$ | $\Delta I$ |
| 51 | 569.1 | 0.4 | 0.13 | 0.06 | | | | |
| 52 | 574.2 | 0.4 | 0.10 | 0.10 | 573.94 | 0.18 | 0.26 | 0.07 |
| 53 | 577.70 | 0.13 | 1.49 | 0.25 | 577.71 | 0.16 | 2.04 | 0.20 |
| 54 | 580.0 | 0.3 | 0.22 | 0.06 | 580.21 | 0.20 | 0.33 | 0.07 |
| 55 | 583.52 | 0.08 | 1.24 | 0.22 | 583.07+ | 0.16 | <2.6 | |
| 56 | 586.07 | 0.09 | 0.76 | 0.16 | 585.68 | 0.16 | 0.81 | 0.07 |
| 57 | 593.28 | 0.10 | 0.63 | 0.08 | 593.00 | 0.16 | 0.80 | 0.05 |
| 58 | 599.33 | 0.18 | 0.19 | 0.04 | 599.00 | 0.18 | 0.26 | 0.02 |
| 59 | 605.52 | 0.15 | 0.79 | 0.13 | 605.13 | 0.16 | 0.99 | 0.07 |
| 60 | 612.13 | 0.12 | 0.43 | 0.06 | 611.60 | 0.16 | 0.56 | 0.04 |
| 61 | 617.8? | 0.5 | 0.07 | 0.05 | 617.1? | 1.4 | 0.02 | 0.02 |
| 62 | 623.5 | 0.7 | 0.17 | 0.06 | 622.85 | 0.18 | 0.24 | 0.03 |
| 63 | 627.1 | 0.3 | 0.57 | 0.16 | 626.97 | 0.19 | 0.88 | 0.09 |
| 64 | 629.1 | 0.4 | 0.29 | 0.10 | 628.85 | 0.31 | 0.31 | 0.07 |
| 65 | 632.4 | 0.5 | 0.13 | 0.06 | 631.84 | 0.24 | 0.20 | 0.03 |
| 66 | | | | | 637.77 | 0.24 | 0.09 | 0.02 |
| 67 | 642.4 | 0.3 | 0.17 | 0.06 | 641.83 | 0.18 | 0.19 | 0.02 |
| 68 | | | | | 646.34? | 0.5 | 0.04 | 0.02 |
| 69 | | | | | 649.18 | 0.33 | 0.07 | 0.02 |
| 70 | 659.7 | 0.3 | 0.26 | 0.05 | 659.13 | 0.18 | 0.35 | 0.03 |
| 71 | 661.8 | 0.4 | 0.14 | 0.05 | 661.86 | 0.21 | 0.26 | 0.05 |
| 72 | 665.09 | 0.13 | 1.27 | 0.19 | 664.90 | 0.16 | 1.54 | 0.07 |
| 73 | | | | | 667.32 | 0.30 | 0.24 | 0.03 |
| 74 | 681.87 | 0.08 | 1.11 | 0.22 | 681.54 | 0.16 | 1.56 | 0.11 |
| 75 | 685.2 | 0.4 | 0.19 | 0.06 | 684.94 | 0.20 | 0.20 | 0.04 |
| 76 | | | | | 692.83 | 0.44 | 0.08 | 0.02 |
| 77 | 695.6 | 0.6 | 0.25 | 0.10 | 696.30 | 0.18 | 0.38 | 0.04 |
| 78 | | | | | 701.80 | 0.34 | 0.13 | 0.02 |
| 79 | 705.07 | 0.15 | 0.83 | 0.19 | 704.79 | 0.17 | 1.19 | 0.06 |
| 80 | | | | | 710.19 | 0.5 | 0.06 | 0.02 |
| 81 | 714.24 | 0.10 | 0.79 | 0.22 | 713.99 | 0.17 | 1.21 | 0.06 |
| 82 | | | | | 721.59 | 0.21 | 0.21 | 0.02 |
| 83 | 724.3? | 0.6 | 0.25 | 0.10 | | | | |
| 84 | 734.6? | 0.4 | 0.13 | 0.06 | 734.80 | 0.19 | 0.25 | 0.02 |
| 85 | 740.9 | 0.6 | 0.19 | 0.06 | 740.83 | 0.19 | 0.27 | 0.02 |
| 86 | | | | | 748.50 | 0.4 | 0.04 | 0.01 |
| 87 | 752.7 | 0.3 | 0.19 | 0.06 | 751.91 | 0.19 | 0.26 | 0.02 |
| 88 | | | | | 766.59 | 0.35 | 0.08 | 0.02 |
| 89 | | | | | 778.24 | 0.5 | 0.07 | 0.02 |
| 90 | | | | | 780.47 | 0.8 | 0.04 | 0.02 |
| 91 | | | | | 786.54? | 0.23 | 0.21 | 0.03 |
| 92 | | | | | 788.82 | 0.32 | 0.12 | 0.02 |
| 93 | 797.2 | 0.4 | 0.41 | 0.16 | 797.50 | 0.17 | 0.83 | 0.04 |
| 94 | | | | | 806.66 | 0.31 | 0.16 | 0.03 |
| 95 | 809.9 | 0.5 | 0.29 | 0.10 | 808.62 | 0.21 | 0.38 | 0.04 |
| 96 | 814.4 | 0.6 | 0.25 | 0.10 | 814.39 | 0.18 | 0.41 | 0.03 |

TABLE I *(Continued)*

| No. | Ge(Li) spectrometer $E$(keV) [a] | $\Delta E$ | $I/100n$ | $\Delta I$ | No. | Ge(Li) spectrometer $E$(keV) [a] | $\Delta E$ | $I/100n$ | $\Delta I$ |
|---|---|---|---|---|---|---|---|---|---|
| 97 | 826.09 | 0.21 | 0.34 | 0.03 | 130 | 1024.1 | 0.3 | 0.47 | 0.07 |
| 98 | 828.54 | 0.21 | 0.36 | 0.03 | 131 | 1031.1 | 0.4 | 0.08 | 0.02 |
| 99 | 833.23 | 0.20 | 0.55 | 0.05 | 132 | 1034.0 | 0.2 | 0.33 | 0.02 |
| 100 | 835.31+ | 0.19 | 0.65 | 0.05 | 133 | 1044.3 | 0.2 | 0.22 | 0.02 |
| 101 | 839.47 | 0.32 | 0.10 | 0.02 | 134 | 1051.8 | 0.3 | 0.16 | 0.02 |
| 102 | 843.09 | 0.26 | 0.19 | 0.03 | 135 | 1054.9 | 0.2 | 0.23 | 0.02 |
| 103 | 845.98 | 0.24 | 0.24 | 0.03 | 136 | 1062.0 | 0.3 | 0.30 | 0.03 |
| 104 | 849.18 | 0.31 | 0.13 | 0.03 | 137 | 1064.3 | 0.8 | 0.05 | 0.02 |
| 105 | 852.82 | 0.24 | 0.18 | 0.03 | 138 | 1073.8 | 0.2 | 0.49 | 0.03 |
| 106 | 869.38 | 0.21 | 0.23 | 0.02 | 139 | 1081.4 | 0.4 | 0.08 | 0.02 |
| 107 | 871.89 | 0.20 | 0.49 | 0.03 | 140 | 1084.6 | 0.5 | 0.06 | 0.02 |
| 108 | 874.35 | 0.21 | 0.24 | 0.03 | 141 | 1091.1 | 0.7 | 0.03 | 0.01 |
| 109 | 885.58 | 0.20 | 0.17 | 0.02 | 142 | 1097.2 | 0.3 | 0.16 | 0.02 |
| 110 | 891.50 | 0.20 | 0.36 | 0.03 | 143 | 1100.9 | 0.2 | 0.41 | 0.03 |
| 111 | 903.35 | 0.39 | 0.05 | 0.01 | 144 | 1105.5 | 0.3 | 0.12 | 0.02 |
| 112 | 907.07 | 0.22 | 0.14 | 0.02 | 145 | 1109.4 | 0.3 | 0.12 | 0.02 |
| 113 | 913.59 | 0.28 | 0.12 | 0.02 | 146 | 1117.1 | 0.3 | 0.20 | 0.02 |
| 114 | 918.45 | 0.20 | 0.19 | 0.02 | 147 | 1125.7 | 0.3 | 0.17 | 0.02 |
| 115 | 928.45 | 0.42 | 0.04 | 0.01 | 148 | 1128.9 | 0.3 | 0.10 | 0.02 |
| 116 | 941.83 | 0.21 | 0.21 | 0.02 | 149 | 1133.4 | 0.3 | 0.16 | 0.02 |
| 117 | 947.24 | 0.37 | 0.07 | 0.01 | 150 | 1145.5 | 0.3 | 0.27 | 0.02 |
| 118 | 951.44 | 0.33 | 0.08 | 0.02 | 151 | 1151.7 | 0.4 | 0.13 | 0.03 |
| 119 | 957.27 | 0.28 | 0.10 | 0.02 | 152 | 1154.3 | 0.4 | 0.13 | 0.02 |
| 120 | 968.01 | 0.21 | 0.67 | 0.04 | 153 | 1158.0 | 0.3 | 0.13 | 0.02 |
| 121 | 976.85 | 0.19 | 0.60 | 0.03 | 154 | 1164.2 | 0.3 | 0.26 | 0.03 |
| 122 | 979.78 | 0.24 | 0.19 | 0.02 | 155 | 1166.8 | 0.4 | 0.11 | 0.02 |
| 123 | 990.66 | 0.20 | 0.28 | 0.02 | 156 | 1171.3 | 0.3 | 0.15 | 0.02 |
| 124 | 996.47 | 0.27 | 0.09 | 0.02 | 157 | 1176.5 | 0.3 | 0.23 | 0.02 |
| 125 | 1001.9 | 0.3 | 0.10 | 0.02 | 158 | 1185.1 | 0.3 | 0.14 | 0.02 |
| 126 | 1004.6 | 0.2 | 0.25 | 0.02 | 159 | 1188.7 | 0.6 | 0.06 | 0.02 |
| 127 | 1013.4 | 0.2 | 0.58 | 0.06 | 160 | 1196.5 | 0.3 | 0.23 | 0.02 |
| 128 | 1015.0 | 0.4 | 0.20 | 0.06 | 161 | 1207.9 | 0.5 | 0.07 | 0.02 |
| 129 | 1022.6 | 0.3 | 0.41 | 0.07 | 162 | 1212.2 | 0.4 | 0.09 | 0.02 |

[a] ?, line questionable; +, energy maybe shifted by overlapping background line.

ness of 2 mm. The neutron flux impinging on the target was $10^6 n/cm^2$ sec. The capture facility, at the end of a neutron guide tube installed at the FRM, has been described in detail.[17,18]

Figure 1 shows that part of the $(n,\gamma)$ spectrum in which most of the lines could still be separated in a satisfactory way. For this spectrum two days of counting time were needed. It contains background lines, which resulted not only from the decay of $^{233}$Th and its decay products, but also, to an appreciable extent, from the decay of $^{232}$Th. To separate the $(n,\gamma)$ lines from the background lines, special runs had to be taken without the neutron beam, both before and immediately after neutron irradiation.

The energies given in Table I have been calibrated with well-known calibration standards: the 121.97 ± 0.03-keV line from $^{57}$Co and the 2223.29 ± 0.07-keV line from $n$ capture in H.[19] The results have been corrected for nonlinearity of the whole system by use of a high-precision Hg pulser. To calibrate the relative efficiency of the Ge(Li) detector, a set of calibrated $\gamma$ sources from the International Atomic Energy Agency (Vienna) has been used, and the intensities given in Table I have been corrected for self-absorption in the target. Relative intensity errors are given in the table. For the absolute intensity calibration the 311-keV line from the decay of $^{233}$Pa (27 day) has been used which is present in the $(n,\gamma)$ spectrum. This intensity was taken from Ref. 15. The error of the absolute intensity calibration is about 25% and has not been included in the $\Delta I$ values.

### C. High-Energy $\gamma$ Rays from Resonance Neutron Capture in $^{232}$Th Measured at Brookhaven

The experiment was performed at the 22-m flight path of the fast-chopper facility at Brookhaven.[20] The sample consisted of a $\frac{1}{4}$-in.-thick plate of natural thorium placed in the standard geometry, and the $\gamma$ rays were detected in a 10-cm$^3$ Ge(Li) diode. Two weeks of beam time were devoted to the experiment. The resulting neutron time-of-flight spectrum is shown in Fig. 2.

The $\gamma$-ray spectra from the four resolved resonances along with that for neutron energies less than 0.2 eV are shown in Fig. 3. Here the $\gamma$-ray energy scale refers to the double-escape peaks. The peak numbers indicate the double-escape peaks, while the full-energy peaks are indicated by the letter F. The numbered peaks are those which appear reasonably strong in at least one of the five spectra.

The $\gamma$-ray energies and absolute intensities are listed in Table II. The energy calibration is based on the background $\gamma$ ray at 2614.47 keV[21] and the separation of one- and two-photon escape peaks. The $\gamma$-ray intensities were determined in a separate experiment by use of composite thin samples of gold and thorium. The intensities of the strong 4214- and 4105-keV $\gamma$ rays in the 23.4-eV thorium resonance were measured relative to the sum of the intensities of $\gamma$ rays with energies exceeding 6.2 MeV in the 4.9-eV resonance of gold. The absolute intensities for gold have been measured as a function of neutron energy from thermal to the 4.9-eV resonance by W. R. Kane, using a diffraction neutron monochromator at the BNL High Flux Beam Reactor. Employing his value[22] of 0.133 photons per capture for the sum of all transitions exceeding 6.2 MeV in the 4.9-eV resonance, we can calculate the absolute intensities

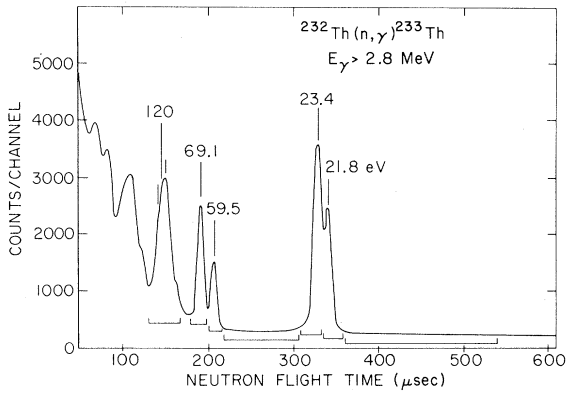


FIG. 2. Neutron time-of-flight spectrum. Capture $\gamma$-ray spectra are measured for the indicated neutron energies.

of Table II. These values are about 30% higher than would be inferred from the older gold measurements of Groshev *et al.*[23] The relative number of neutrons captured in each resonance was calculated from the measured relative neutron flux and the known resonance parameters by use of the thorium values of Bhat and Chrien[24] and the gold parameters of Wood.[25] Corrections for $\gamma$-ray detection efficiency were applied.

Fluctuations of the $\gamma$ rays were found to be consistent with the Porter-Thomas distribution[26] of radiative widths. This strongly suggests that the statistical model of neutron capture may be used to evaluate the thorium $\gamma$-ray spectra for shielding calculations.

The combination of the high-energy $\gamma$ lines with the level energies in $^{233}$Th results in a $Q$ value of the $(n,\gamma)$ reaction of $4786.5 \pm 2.0$ keV. The newest Atomic Mass Table[27] gives the value $4787 \pm 5$ keV.

It is surprising that no $M1$ transitions from the $\frac{1}{2}^+$ capture state to the $\frac{1}{2}^+$ ground state and to the $\frac{3}{2}^+$ state at 16 keV were observed although corresponding transitions have been seen in $^{235}$U[28] and $^{239}$U.[29,30] Kernbach, Fiebiger, and Stelzer[4] detected these transitions in thermal-neutron capture in $^{233}$Th. The upper intensity limits in this experiment from the transitions to the ground state and 16-keV state are given in Table II. Porter-Thomas fluctuations seem to cause the failure to observe these transitions in the four resonances.

The summed intensity of a $\gamma$ transition ($\sum I_j$) over resonances gives some indication of the multipolarity of the transition, and thus an indication of the spin and parity of the populated level.[31] According to Bollinger and Thomas,[27] $M1$ transitions are on the average a factor of 6 weaker than $E1$ transitions and for $E2$ transitions a factor of 45. For one multipolarity, a 70% intensity variation is expected for the average over four resonances due to Porter-Thomas fluctuations.[31] Assuming that transitions with $\sum I_j > 32$ are $E1$ transitions, one gets an average $\sum I_j(E1) = 60 \pm 42$. With this value one calculates $\sum I_j(M1) = 11 \pm 8$ and $\sum I_j(E2) = 1 \pm 1$. These intensity estimates were used to give tentative spin and parity assignments to levels above 500 keV.

### D. $(d, p)$ Reaction Measured at Argonne

The data on the reaction $^{232}$Th$(d, p)^{233}$Th were taken with the Enge split-pole magnetic spectrograph[32] at the tandem Van de Graaff accelerator. A bombarding energy of 12 MeV was used. The energy scale of the spectrograph was calibrated with $\alpha$ particles from a $^{210}$Po source, whose energy was taken to be $5.3045 \pm 0.0005$ MeV. The tar-

get was prepared by evaporating natural thorium metal from a tantalum boat. The data were recorded on nuclear emulsions, and the tracks were counted with the Argonne automatic nuclear-emulsion scanner.[33] A few peaks were hand counted to check the automatic scanner. The resulting spectra were analyzed with the automatic spectrum-decomposition program AUTOFIT.[34]

The data on the $(d,p)$ reaction (Table III and Fig. 4) were recorded at three angles (90, 135, and 150°), since it was known from previous studies[35,36] of $(d,p)$ reactions on actinide nuclei that information about the $l$ value of the captured neutron could be obtained from the ratio $d\sigma(90°)/d\sigma(150°)$.

Absolute differential cross sections were measured by comparing the yield in the $(d,p)$ reaction with the yield of deuterons elastically scattered from the target. The deuterons were recorded by a silicon solid-state detector mounted at 90° to the beam direction. The ratio of the elastic scattering cross section to that for pure Coulomb scattering was taken to be 0.7 on the grounds that the measurement[37] of the 90° yields in the scattering

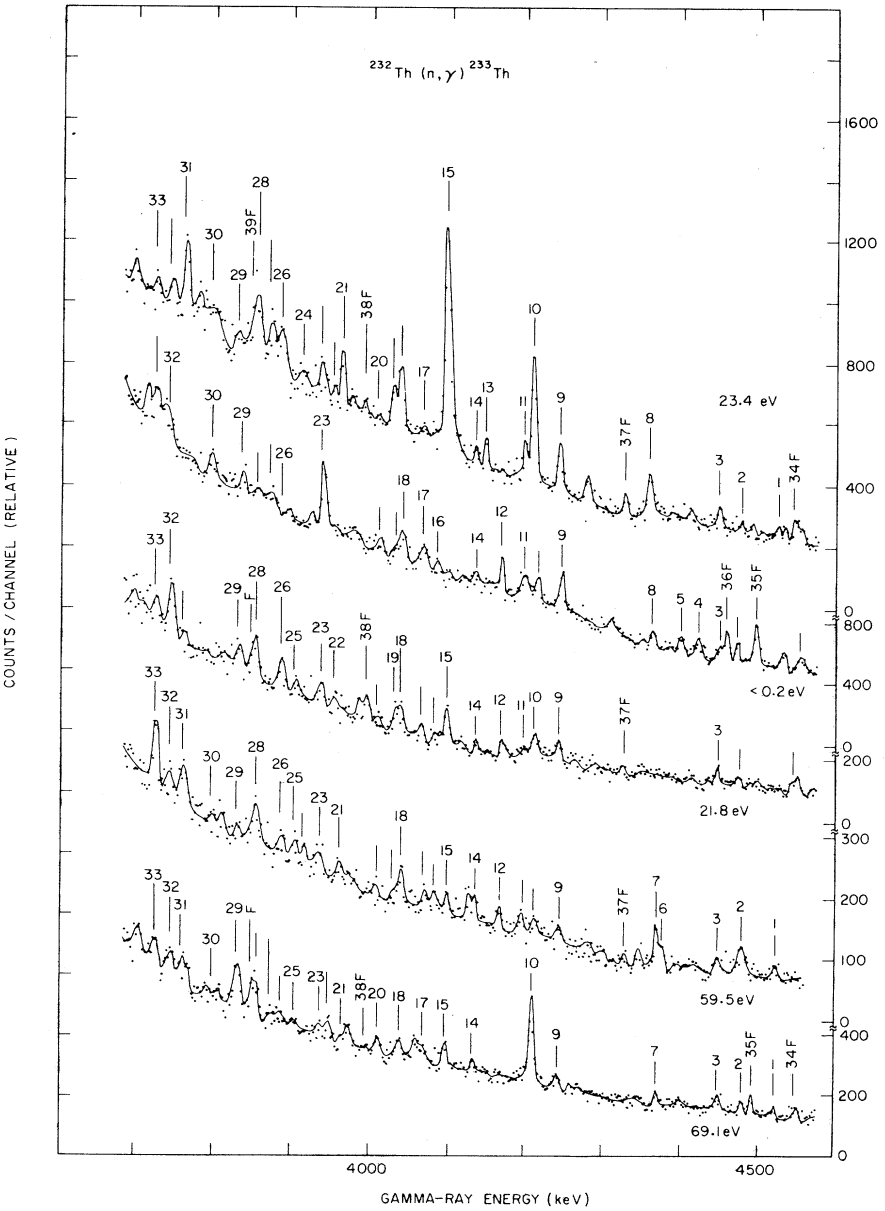


FIG. 3. $\gamma$ spectra from capture of neutrons with different energies.

of 12-MeV deuterons by $^{238}$U had given $0.70 \pm 0.03$ for this ratio. The $^{232}$Th$(d,p)^{233}$Th $Q$ value was determined to be $2.567 \pm 0.007$ MeV, corresponding to a neutron binding energy of $4792 \pm 7$ keV, which is in good agreement with the value in the previous section.

### 3. LEVEL SCHEME

A level scheme of $^{233}$Th (Fig. 5) was constructed using all experimental information, some theoretical predictions, and the similarity to the $^{235}$U level scheme.[28,35,38] The left side of the scheme

TABLE II. $\gamma$-ray energies and intensities from resonant neutron capture in $^{232}$Th.

| Peak No. | $E_\gamma$ (keV) | $E_{ex}$ [a] (keV) | $I_j$, photons per 1000 captures <0.2 eV | 21.8 eV | 23.4 eV | 59.5 eV | 69.1 eV | $\sum I_j$ |
|---|---|---|---|---|---|---|---|---|
| | (4786.5) | 0 | | | | | | <7.9 |
| | (4769.7) | 16.8 | | | | | | <10.5 |
| 1 | 4525.9 ± 2.0 | 260.6 | 3.7 ± 1.1 | <2.8 | 2.8 ± 1.1 | <3.4 | 3.0 ± 1.7 | 10.3 |
| 2 | 4477.0 | 309.5 | 2.8 ± 1.1 | 2.4 ± 1.1 | 2.1 ± 1.1 | 14.3 ± 2.4 | 5.5 ± 1.7 | 27.1 |
| 3 | 4451.0 | 335.5 | 2.4 ± 1.1 | 3.8 ± 1.3 | 4.5 ± 1.1 | 8.5 ± 2.8 | 9.2 ± 2.1 | 28.4 |
| 4 | 4419.5 [c] | 367.0 | 4.5 ± 1.1 | <2.8 | <2.1 | <3.4 | <3.4 | 4.5 |
| 5 | 4398.2 [c] | 388.3 | 4.7 ± 1.1 | <2.8 | <2.1 | <3.1 | <3.4 | 4.7 |
| 6 | 4380.7 | 405.8 | <2.8 | <2.8 | <2.1 | 6.8 ± 2.1 | <3.4 | 6.8 |
| 7 | 4372.7 | 413.8 | <2.8 | <2.8 | <2.1 | 12.6 ± 2.1 | 6.2 ± 2.1 | 18.8 |
| 8 | 4362.2 [c] | 424.3 | 4.1 ± 1.1 | <2.8 | 7.9 ± 1.1 | 4.1 ± 2.4 | <3.4 | 16.1 |
| 9 | 4246.7 | 539.8 | 7.5 ± 1.3 | 6.8 ± 1.3 | 8.2 ± 1.1 | 5.8 ± 2.4 | 7.9 ± 2.1 | 36.2 |
| 10 | 4214.4 [c] | 572.1 | 6.2 ± 1.3 | 5.1 ± 1.7 | 21.8 ± 1.1 | 4.7 ± 2.4 | 40.4 ± 4.7 | 78.2 |
| 11 | 4202.4 | 584.1 | 8.2 ± 1.3 | 4.1 ± 1.7 | 7.2 ± 1.1 | 8.5 ± 2.4 | <3.4 | 28.0 |
| 12 | 4172.4 [c] | 614.1 | 6.2 ± 1.3 | 3.4 ± 1.1 | <2.1 | 8.2 ± 2.1 | <3.4 | 17.8 |
| 13 | 4153.7 | 632.8 | <2.8 | <2.8 | 5.1 ± 1.1 | <3.4 | <3.4 | 5.1 |
| 14 | 4141.0 | 645.5 | <2.8 | 3.8 ± 1.1 | 3.4 ± 1.1 | 8.9 ± 2.1 | 4.5 ± 2.1 | 20.6 |
| 15 | 4104.9 | 681.6 | <2.8 | 17.1 ± 2.1 | 41.0 ± 2.1 | 8.2 ± 2.1 | 12.4 ± 2.8 | 78.7 |
| 16 | 4090.9 | 695.6 | 3.0 ± 1.3 | <2.1 | <2.1 | 6.8 ± 2.8 | <3.4 | 9.8 |
| 17 | 4073.0 | 713.5 | 7.5 ± 1.3 | 5.5 ± 1.1 | <2.1 | 6.2 ± 2.8 | 14.7 ± 3.4 | 33.9 |
| 18 | 4045.8 | 740.7 | 7.2 ± 1.3 | 3.4 ± 1.3 | 10.9 ± 1.1 | 12.6 ± 2.1 | 14.7 ± 2.8 | 48.8 |
| 19 | 4036.6 | 749.9 | 3.4 ± 1.3 | 1.7 ± 1.1 | 6.4 ± 1.1 | 2.4 ± 1.7 | <2.8 | 13.9 |
| 20 | 4019.0 | 767.5 | 1.3 ± 1.3 | 1.1 ± 1.1 | 1.3 ± 1.3 | 1.7 ± 1.7 | 9.2 ± 2.1 | 14.6 |
| 21 | 3967.9 | 818.6 | <2.8 | <2.8 | 10.7 ± 2.1 | 6.4 ± 1.7 | 2.8 ± 2.1 | 19.9 |
| 22 | 3956.0 | 830.5 | <2.8 | 3.0 ± 1.7 | 2.1 ± 1.3 | <3.4 | 7.5 ± 2.1 | 12.6 |
| 23 | 3946.0 | 840.5 | 17.1 ± 2.1 | 11.3 ± 2.1 | 5.8 ± 1.3 | 9.6 ± 2.4 | <3.4 | 43.8 |
| 24 | 3925.5 | 861.0 | <2.8 | <2.8 | 3.0 ± 1.3 | 6.8 ± 1.7 | <3.4 | 9.8 |
| 25 | 3912.2 | 874.3 | <2.8 | 4.1 ± 1.3 | <2.8 | 8.9 ± 1.7 | 2.8 ± 2.1 | 15.8 |
| 26 | 3894.7 | 891.8 | <2.8 | 9.2 ± 1.3 | 11.3 ± 1.3 | 6.8 ± 1.7 | 5.1 ± 2.1 | 32.4 |
| 27 | 3882.9 | 903.6 | 2.8 ± 2.1 | <2.8 | 12.0 ± 1.3 | <3.4 | 4.7 ± 2.1 | 19.5 |
| 28 | 3862.4 | 924.1 | <2.8 | 18.4 ± 2.1 | 18.1 ± 2.8 | 18.8 ± 3.4 | 13.7 ± 3.0 | 69.0 |
| 29 | 3839.8 | 946.7 | 4.1 ± 2.1 | 9.6 ± 2.1 | 6.4 ± 2.8 | 6.4 ± 2.1 | 23.9 ± 3.0 | 50.4 |
| 30 | 3804.9 | 981.6 | 6.4 ± 1.7 | <2.8 | 6.8 ± 2.8 | <3.4 | <3.4 | 13.2 |
| 31 | 3774.0 | 1012.5 | <2.8 | <2.8 | 14.3 ± 1.1 | 21.2 ± 4.1 | 16.0 ± 3.0 | 51.5 |
| 32 | 3755.5 | 1031.0 | 6.2 ± 1.3 | 21.6 ± 1.3 | 5.1 ± 1.1 | 8.2 ± 2.1 | 17.8 ± 2.8 | 58.9 |
| 33 | 3736.3 | 1050.2 | 11.6 ± 1.7 | 11.6 ± 1.3 | 3.8 ± 1.1 | 21.8 ± 2.4 | 17.1 ± 2.4 | 65.9 |
| 34F [b] | 3524.0 | 1262.5 | 12.4 ± 3.0 | 8.2 ± 3.0 | 7.2 ± 3.0 | <4.7 | <6.2 | 27.8 |
| 35F | 3472.2 | 1314.3 | 28.7 ± 3.4 | <3.4 | <3.4 | <4.7 | 21.6 ± 5.1 | 50.3 |
| 36F | 3434.5 | 1352.0 | 18.4 ± 3.0 | <3.0 | <3.0 | <4.7 | <6.2 | 18.4 |
| 37F | 3308.2 | 1478.3 | <6.8 | 1.7 ± 1.3 | 9.2 ± 2.8 | 5.1 ± 2.8 | <6.2 | 16.0 |
| 38F | 2983.0 | 1803.5 | <6.8 | 21.2 ± 2.8 | <3.0 | 6.8 ± 4.1 | <6.2 | 28.0 |
| 39F | 2841.5 | 1945.0 | 8.5 ± 5.1 | 34.2 ± 6.8 | 51.3 ± 10.3 | <10.3 | 54.7 ± 13.7 | 148.7 |
| Sum of all $\gamma$ rays | | | 179.7 <236.9 | 212.3 <254.4 | 289.7 <316.6 | 247.1 <295.3 | 315.4 <380.4 | |

[a] Calculated with $Q_n = 4786.5$ keV ± 2 keV.

[b] F indicates full-energy peak.

[c] *Note added in proof*: Peaks 4, 5, 8, 10, and 12 are contaminated by an undetermined full-energy peak contribution from lines located 1022 keV below the listed energies; hence their intensities must be regarded as upper limits. We are indebted to Dr. Jean Kern, U. Fribourg, for this information.

TABLE III. Excitation energies of levels in $^{233}$Th, differential cross sections in $(d, p)$ reaction, and orbital assignments.

| Excitation energy (keV) | $d\sigma/d\Omega$ [a] at 150° ($\mu$b/sr) | $R = \frac{d\sigma(90°)}{d\sigma(150°)}$ | Assignment $I$ | Assignment Orbital |
|---|---|---|---|---|
| 0 | 47 | 2.8 | $\frac{1}{2}$ | $\frac{1}{2}^+[631\downarrow]$ |
| 16.1 ± 0.5 | 98 | 2.2 | $\frac{3}{2}$ | $\frac{1}{2}^+[631\downarrow]$ |
| 53.5 ± 0.5 | 4 | ~2 | $\frac{5}{2}$ | $\frac{1}{2}^+[631\downarrow]$ |
| 92.5 ± 1.5 | 13 | ~2 | $\frac{7}{2}$ | $\frac{1}{2}^+[631\downarrow]$ |
| 106.9 ± 1 | 128 | 1.2 | $\frac{9}{2}$ | $\frac{5}{2}^+[622\uparrow]$ |
| 159.0 ± 1 | 59 | 1.1 | $\frac{9}{2}$ | $\frac{1}{2}^+[631\downarrow]$ |
| 178 ± 2 | 6 | ~0.4 | $\frac{11}{2}$ | $\frac{5}{2}^+[622\uparrow]$ |
| 220 ± 2 | 11 | ~0.3 | $\frac{11}{2}$ | $\frac{1}{2}^+[631\downarrow]$ |
| 252.3 ± 0.5 | 30 | 0.38 | $(\frac{15}{2}$ | $\frac{7}{2}^-[743\uparrow])$ |
| 278 ± 2 | 11 | ~0.5 | $\frac{7}{2}$ | $\frac{7}{2}^+[624\downarrow]$ |
| 326.0 ± 1 | 87 | 1.2 | $\frac{9}{2}$ | $\frac{7}{2}^+[624\downarrow]$ |
| (336) ± 5 | 5 | b | $\frac{3}{2}$ | $\frac{3}{2}^+[631\uparrow]$ |
| 370.6 ± 1 | 23 | 1.6 | $\frac{5}{2}$ | $\frac{3}{2}^+[631\uparrow]$ |
| 388.5 ± 1 | 10 | ~0.6 | $\frac{11}{2}$ | $\frac{7}{2}^+[624\downarrow]$ |
| | | | $\frac{9}{2}$ | $\frac{5}{2}^+[633\downarrow]$ |
| 410 ± 1.5 | 19 | 1.1 | | |
| (443) ± 5 | 6 | ~0.5 | | |
| 464 ± 3 | 6 | ~0.5 | $\frac{11}{2}$ | $\frac{5}{2}^+[633\downarrow]$ |
| 480.9 ± 1 | 19 | 0.66 | $\frac{9}{2}$ | $\frac{3}{2}^+[631\uparrow]$ |
| 538 ± 2 | 28 | 1.7 | $(\frac{1}{2}$ | $\frac{1}{2}^-[501\downarrow])$ |
| 582 ± 1.5 | 49 | 2.0 | $(\frac{3}{2}$ | $\frac{1}{2}^-[501\downarrow])$ |
| 610 ± 1.5 | 6 | ~1 | | |
| 627.8 ± 2 | 55 | 1.7 | | |
| 680.6 ± 1 | 22 | 2.6 | | |
| 691.2 ± 1.5 | 16 | ~1 | | |
| 710.6 ± 1.5 | 8 | ~0.8 | | |
| 725.8 ± 1 | 32 | 1.6 | | |
| 753.4 ± 1.5 | 7 | ~1 | | |
| 766.8 ± 2 | 16 | ~2 | | |
| 796 ± 3 | 8 | b | | |
| 812 ± 3 | 16 | ~1 | | |
| 846 ± 3 | ~46 | b | | |
| (855) ± 5 | ~14 | b | | |
| 873 ± 4 | 4 | b | | |
| 887 ± 3 | 18 | ~0.7 | | |
| 900 ± 3 | 11 | ~0.5 | | |
| 924 ± 4 | 12 | 2.4 | | |
| 945 ± 4 | 6 | ~1 | | |
| 954 ± 4 | 6 | ~1 | | |
| 973 ± 4 | 16 | 1.2 | | |
| 991 ± 3 | 20 | ~1 | | |
| 1026 ± 3 | 65 | 1.1 | | |
| 1038 ± 4 | 16 | ~1.2 | | |
| 1046 ± 4 | 8 | ~1.5 | | |
| 1073 ± 5 | 9 | ~1 | | |
| 1101 ± 3 | 163 | 1.5 | | |
| 1116 ± 5 | 16 | b | | |
| 1130 ± 3 | 62 | ~0.8 | | |
| 1152 ± 4 | 89 | 1.6 | | |
| 1164 ± 4 | 49 | ~1.5 | | |
| (1170) ± 5 | 13 | b | | |
| 1178 ± 4 | 65 | ~0.8 | | |
| 1190 ± 5 | 24 | ~1.3 | | |
| 1219 ± 5 | 18 | ~1 | | |
| 1236 ± 4 | 10 | ~1 | | |
| 1258 ± 4 | 49 | 1.8 | | |
| 1265 ± 4 | 52 | 1.8 | | |
| 1280 ± 4 | 48 | 2.1 | | |
| 1290 ± 5 | 27 | 1.5 | | |
| 1302 ± 4 | 32 | 1.8 | | |
| 1316 ± 5 | 20 | b | | |
| 1331 ± 4 | 26 | 1.3 | | |
| 1344 ± 5 | 15 | b | | |
| 1367 ± 5 | 12 | 1.3 | | |
| 1387 ± 4 | 26 | 1.5 | | |
| 1394 ± 4 | 24 | 1.5 | | |
| 1402 ± 5 | 18 | b | | |
| 1430 ± 4 | 27 | 1.3 | | |

[a] The uncertainty in the cross sections of the strongly excited states is about 10%.
[b] The yield is too low to obtain a meaningful ratio.

shows the rotational structure of the levels below 500 keV together with the excitation energies from the $(d,p)$ reaction and from high-energy capture $\gamma$ rays. The right side of the scheme shows the low-energy capture $\gamma$ rays arranged mainly by the Ritz energy-combination principle and by considering the level structure found with the $(d,p)$ reaction. There is a small probability that a transition is fitted into the scheme incorrectly. Although many more levels could be placed in the scheme by energy combination, only those were accepted which had a high degree of certainty. The level energies and errors on the right side of the scheme were calculated with a least-squares program which fits the level energies to all transition energies. The spin and parity assignments for the levels below 500 keV were made according to the Nilsson configurations of these levels with some help from the $d\sigma(90°)/d\sigma(150°)$ ratios in the $(d,p)$ yields. The tentative spin and parity assignments of the levels above 500 keV were estimated from the decay properties and the population by high-energy $\gamma$ rays.

### A. Rotational Bands

#### [631↓] *Ground-State Band*

The Nilsson model and the comparison with $^{235}$U suggest that the ground state of $^{233}$Th has the configuration $\frac{1}{2}^+[631\downarrow]$ or $\frac{7}{2}^-[743\uparrow]$; $\frac{5}{2}^+[622\uparrow]$ might be possible, too. The spin and parity $\frac{1}{2}^+$ of the ground state of $^{233}$Th was determined by the log$ft$ values of the different $\beta$-decay branches to levels in $^{233}$Pa.[5,39-41] The proton line with the highest energy in the $(d,p)$ spectrum leads to a level with a $Q$ value of $2.567 \pm 0.007$ MeV. This level has been identified as the $\frac{1}{2}^+[631\downarrow]$ state by spectroscopic factor, measured $l$ value, and comparison with the reaction $^{234}$U$(d,p)^{235}$U. The ground-state $Q$ value from the 1971 Mass Tables[27] is $2.562 \pm 0.005$ MeV. Therefore, we assign the ground state of $^{233}$Th to the configuration $\frac{1}{2}^+[631\downarrow]$.

The $I = \frac{1}{2}, \frac{3}{2}, \frac{5}{2}, \frac{7}{2}, \frac{9}{2}$, and $\frac{11}{2}$ members of this band are seen in the $(d,p)$ reaction. The $\frac{1}{2}$, $\frac{3}{2}$, $\frac{5}{2}$, and $\frac{7}{2}$ levels are populated appreciably by low-energy $\gamma$ rays. The decoupling parameter of this band calculated with the lowest levels is $a = -0.147$. The Coriolis fitting program (see Sec. 4 A) gives the value $a = -0.142$. Theoretical values for the decoupling parameters are: $-0.88$ (Nilsson model without $\epsilon_4$),[42] $-0.131$ (Nilsson model with $\epsilon_4$),[43,44] and $-0.8$ (Malov and Soloviev).[45]

#### [622↑] *Band*

One of the most intense peaks in the $(d,p)$ spectrum corresponds to a level at 106.9 keV. The 90 to 150° cross-section ratio suggests a spin $\frac{7}{2}$ or $\frac{9}{2}$. Comparison with $^{235}$U indicates that this is the $\frac{9}{2}[622\uparrow]$ level. The $\frac{5}{2}$ band head at 5.98 keV is populated by low-energy $\gamma$ rays. The corresponding $(d,p)$ peak is covered by the $\frac{1}{2}$ and $\frac{3}{2}$ members of the ground-state band. The $\frac{11}{2}$ member was observed in the $(d,p)$ reaction at 178 keV. Spectroscopic factors are in good agreement with this assignment. The excitation energy of the $[622\uparrow]$ band head decreases from 280 keV in $^{237}$Pu[46,47] to 129 keV in $^{235}$U.[35] This tendency suggests that this configuration is expected close to the ground state in $^{233}$Th. The $\frac{7}{2}^+[622\uparrow]$ state could be identified tentatively at 50.28 keV by one $\gamma$ transition, in good agreement with the level energy predicted by the Coriolis-mixing calculation (see Table IV).

#### [631↑] *Band*

The low-energy and high-energy $\gamma$ transitions yield levels at 335.92 and 371.22 keV. A tentative level is placed at 421.24 keV. The rotational for-

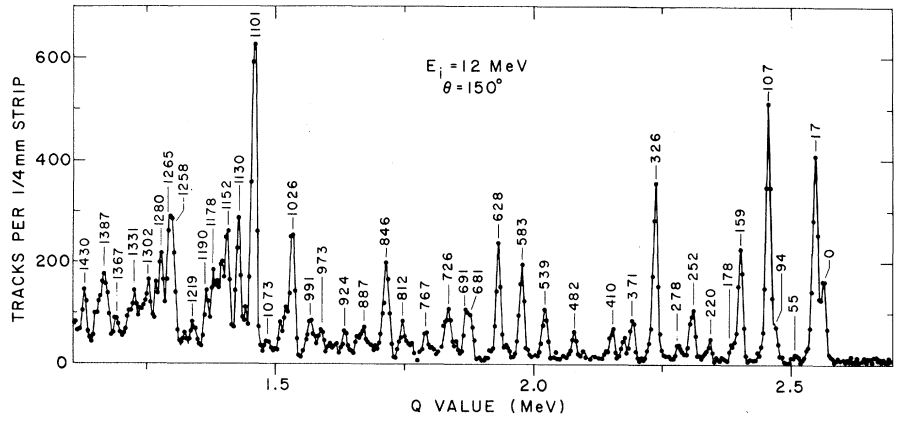


FIG. 4. Spectrum of protons from the reaction $^{232}$Th$(d,p)^{233}$Th observed at 150°. (Peaks labeled in keV.)

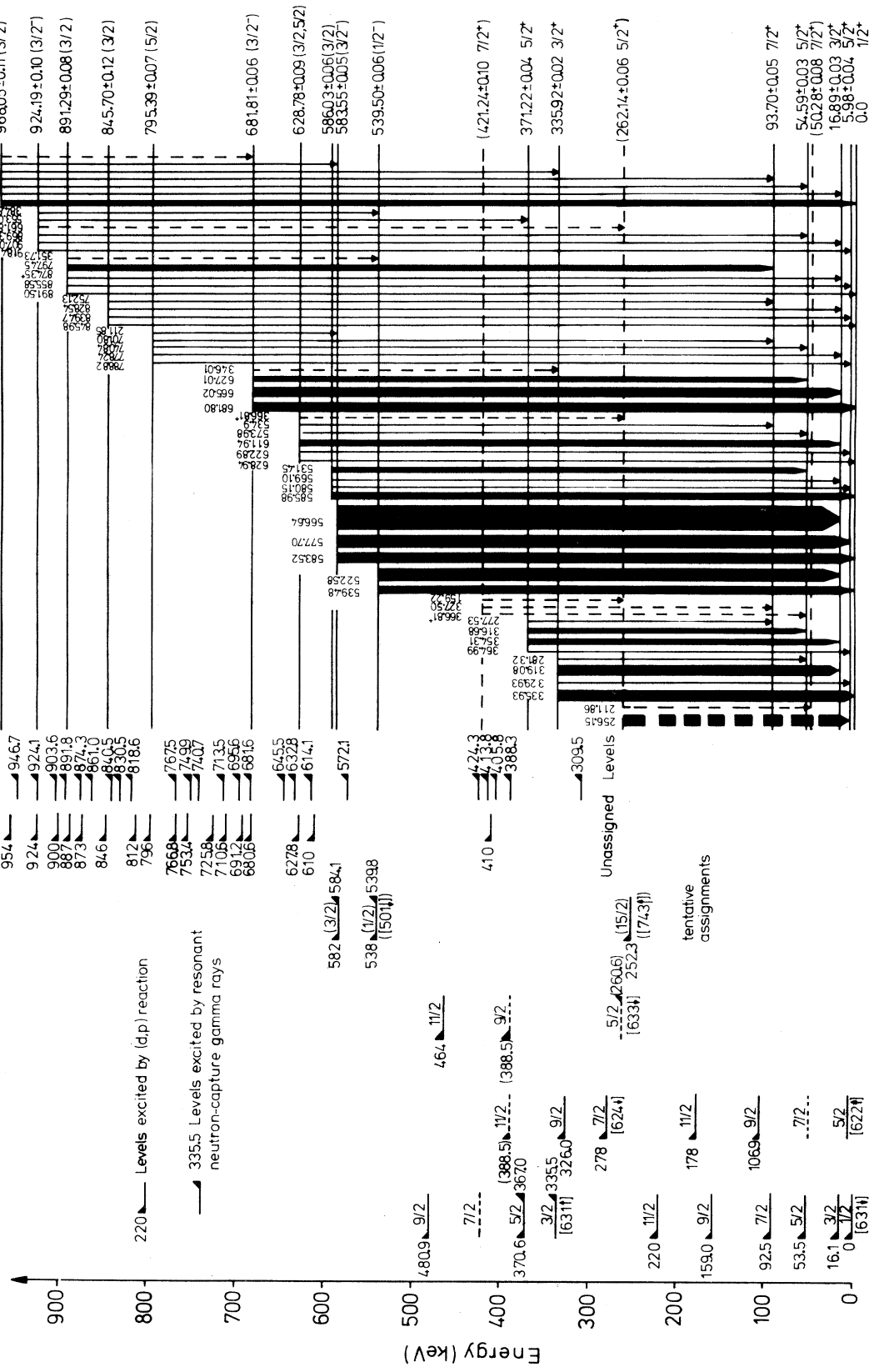


FIG. 5. Level scheme of $^{233}$Th. The $\gamma$-transition energies are averaged values from crystal- and Ge(Li)-spectrometer measurements.

TABLE IV. Spectroscopic factors $S_{jl}$ of the rotational bands.

| Rot. band | Energy $(n,\gamma)$ (keV) | Energy $(d,p)$ (keV) | Energies calculated with fitting program (keV) | $d\sigma/d\Omega$ $(d,p)$ at 150° ($\mu$b/sr) | $R_{exp} = \frac{d\sigma(90°)}{d\sigma(150°)}$ | $\sigma_{DWBA}$ at 150° | $R_{theor} = \frac{d\sigma(90°)}{d\sigma(150°)}$ | $S_{lj,\,exp}$ | $S_{jl}$, theory: Without Coriolis mixing, Without $\epsilon_4$ | $S_{jl}$, theory: Without Coriolis mixing, With $\epsilon_4$ | $S_{jl}$, theory: With Coriolis mixing, Without $\epsilon_4$ | $S_{jl}$, theory: With Coriolis mixing, With $\epsilon_4$ |
|---|---|---|---|---|---|---|---|---|---|---|---|---|
| $\frac{1}{2}$[631↓] | 0.0 | 0.0 | 0.0 | 47 | 2.8 | 301 | 2.3 | 0.052 | 0.106 | 0.095 | 0.106 | 0.095 |
| $\frac{3}{2}$ | 16.89 ± 0.04 | 16.1 ± 0.5 | 16.67 | 98 | 2.2 | 202 | 1.6 | 0.081 | 0.112 | 0.070 | 0.113 | 0.070 |
| $\frac{5}{2}$ | 54.59 ± 0.03 | 53.5 ± 0.5 | 53.63 | 4 | ~2 | 206 | 1.6 | 0.0022 | 0.014 | 0.026 | 0.0144 | 0.026 |
| $\frac{7}{2}$ | 93.70 ± 0.05 | 92.5 ± 1.5 | 92.53 | 13 | ~2 | 76 | 1.1 | 0.014 | 0.026 | 0.0080 | 0.0256 | 0.0080 |
| $\frac{9}{2}$ | | 159.0 ± 1 | 159.05 | 59 | 1.1 | 78 | 1.0 | 0.050 | 0.027 | 0.039 | 0.0266 | 0.0388 |
| $\frac{11}{2}$ | | 220 ± 2 | 220.18 | 11 | ~0.3 | 13 | 0.5 | 0.047 | 0.022 | 0.032 | 0.0232 | 0.0337 |
| $\frac{13}{2}$ | | | | | | 14 | 0.5 | | 0.0017 | 0.0023 | | |
| $\frac{5}{2}$[622↑] | 5.98 ± 0.04 | | 5.20 | <20 | | 201 | 1.6 | <0.01 | 0.012 | 0.0006 | 0.0133 | 0.0008 |
| $\frac{7}{2}$ | (50.28 ± 0.08) | | 50.13 | <4 | | 74 | 1.1 | <0.005 | 0.0001 | 0.006 | 0.0006 | 0.0079 |
| $\frac{9}{2}$ | | 106.9 ± 1 | 107.80 | 128 | 1.2 | 76 | 1.1 | 0.112 | 0.112 | 0.034 | 0.108 | 0.0273 |
| $\frac{11}{2}$ | | 178 ± 2 | 178.13 | 6 | ~0.4 | 13 | 0.5 | 0.026 | 0.039 | 0.105 | 0.0655 | 0.130 |
| $\frac{13}{2}$ | | | | | | 14 | 0.5 | | 0.0049 | 0.0002 | | |
| $\frac{5}{2}$[633↓] | (262.14 ± 0.06) | | 262.17 | | | 230 | 1.6 | | 0.0013 | 0.0017 | 0.0010 | 0.0015 |
| $\frac{7}{2}$ | | | 324.05 | <20 | | 83 | 1.0 | <0.02 | 0.0049 | 0.0022 | 0.0000 | 0.0003 |
| $\frac{9}{2}$ | | (388.5 ± 1) | 391.92 | (10) | (~0.6) | 86 | 1.0 | (0.0078) | 0.0081 | 0.027 | 0.0034 | 0.0260 |
| $\frac{11}{2}$ | | 464 ± 3 | 470.92 | 6 | ~0.5 | 14 | 0.5 | 0.024 | 0.021 | 0.0055 | 0.0136 | 0.0000 |
| $\frac{13}{2}$ | | | | | | 14 | 0.5 | | 0.0013 | 0.0023 | | |
| $\frac{7}{2}$[624↓] | | 278 ± 2 | 278.59 | 11 | ~0.5 | 82 | 1.0 | 0.011 | 0.0079 | 0.0017 | 0.0130 | 0.0037 |
| $\frac{9}{2}$ | | 326.0 ± 1 | 325.03 | 87 | 1, 2 | 83 | 1.0 | 0.070 | 0.023 | 0.153 | 0.0367 | 0.167 |
| $\frac{11}{2}$ | | 388.5 ± 1 | 385.66 | (10) | (~0.6) | 14 | 0.5 | (0.040) | 0.122 | 0.015 | 0.110 | 0.0123 |
| $\frac{13}{2}$ | | | | | | 14 | 0.5 | | 0.0032 | 0.0037 | | |
| $\frac{3}{2}$[631↑] | 335.92 ± 0.02 | (336) | 335.73 | 5 | | 240 | 1.6 | 0.0035 | 0.0000 | 0.0002 | 0.0000 | 0.0002 |
| $\frac{5}{2}$ | 371.22 ± 0.04 | 370.6 ± 1 | 370.15 | 23 | 1.6 | 242 | 1.6 | 0.0106 | 0.0061 | 0.0011 | 0.0050 | 0.0011 |
| $\frac{7}{2}$ | (421.24 ± 0.1) | | 418.46 | <5 | | 86 | 1.0 | <0.005 | 0.0016 | 0.0047 | 0.0010 | 0.0027 |
| $\frac{9}{2}$ | | 480.9 ± 1 | 480.75 | 19 | 0.66 | 88 | 1.0 | 0.014 | 0.016 | 0.0082 | 0.0042 | 0.0025 |

TABLE IV (*Continued*)

| Rot. band | Energy $(n,\gamma)$ (keV) | Energy $(d,p)$ (keV) | Energies calculated with fitting program (keV) | $d\sigma/d\Omega$ $(d,p)$ at 150° ($\mu$b/sr) | $R_{exp}=\frac{d\sigma(90°)}{d\sigma(150°)}$ | $\sigma_{DWBA}$ at 150° | $R_{theor}=\frac{d\sigma(90°)}{d\sigma(150°)}$ | $S_{jl}$, exp | $S_{jl}$, theory Without Coriolis mixing Without $\epsilon_4$ | $S_{jl}$, theory Without Coriolis mixing With $\epsilon_4$ | $S_{jl}$, theory With Coriolis mixing Without $\epsilon_4$ | $S_{jl}$, theory With Coriolis mixing With $\epsilon_4$ |
|---|---|---|---|---|---|---|---|---|---|---|---|---|
| $\frac{11}{2}^-$ | | | 557.13 | <7 | | 15 | 0.5 | <0.03 | 0.014 | 0.022 | 0.0061 | 0.0046 |
| $\frac{13}{2}$ | | | | | | 15 | 0.5 | | 0.0014 | 0.0003 | | |
| $\frac{15}{2}$[743↑] | | (252.3 ± 0.5) | | (30) | (0.38) | 6.9 | 0.3 | (0.181) | 0.089 | 0.090 | | |
| $\frac{1}{2}$[501↓] | (539.50 ± 0.06) | (538 ± 2) | | (28) | (1.7) | 295 | 1.8 | (0.032) | 0.040 | 0.043 | | |
| $\frac{3}{2}$ | (583.55 ± 0.05) | (582 ± 1.5) | | (49) | (2.0) | 300 | 1.3 | (0.027) | 0.0043 | 0.0027 | | |

mula and $\gamma$ branching ratios (see Sec. 4 B) indicate that these levels form a $K=\frac{3}{2}$ rotational band. The $(d,p)$ population of the $\frac{5}{2}$ level at 370.6 keV and the $\frac{9}{2}$ level at 480.9 keV suggest the [631↑] assignment for this band, which is expected as a hole state at about this excitation energy.

### [633↓] *and* [624↓] *Bands*

The [633↓] and [624↓] bands originate from the $g_{9/2}$ state and are connected by a large Coriolis matrix element. In $^{233}$Th the first state is a hole state, the other one a particle state. We assign the 278- and 326.0-keV $(d,p)$ levels to the $\frac{7}{2}$ and $\frac{9}{2}$[624↓] configurations and the 464-keV $(d,p)$ level to the $\frac{11}{2}$[633↓] configuration. The 388.5-keV $(d,p)$ level is probably a doublet consisting of the $\frac{11}{2}$[624↓] and $\frac{9}{2}$[633↓] configurations. The spectroscopic factors, the measured $l$ values, and the Coriolis calculation (see Sec. 4 A) support this identification. The Coriolis calculation shows that both bands have nearly the same $E_0$ (about 200 keV) in the rotational formula $E=E_0+AI(I+1)$. This means that the energy spacing of these bands is strongly perturbed. The wave functions of these bands seem to be mixed nearly 50%.

There is a problem with this assignment at 260.6 keV of the $\frac{5}{2}$[633↓] level, the only level of these two bands which should have strong $\gamma$ transitions to lower levels. This $\frac{5}{2}$ level should not be observed in the $(d,p)$ reaction, but might be weakly populated by a direct $E2$ transition in neutron capture. The Nilsson model predicts that it decays mainly to the $\frac{5}{2}$[622↓] level. The 256.16-keV transition is the main candidate for the decay of this level. If the 256.16-keV transition is added to the 5.98-keV level, the predicted level energy would be 262.14 keV, in good agreement with an observed 260.6-keV level from $(n_{res},\gamma)$. But there are no other good energy combinations observed for this level. Possibly, the 211.86-keV transition leads to the very tentative 50.28-keV level ($\frac{7}{2}$[622↑]). The transition rates of the 256.16- and 211.86-keV transitions agree with theoretical predictions (Table VII).

### *Tentative* [743↑] *and* [501↓] *Bands*

The 252.3-keV $(d,p)$ level has a high $l$ value ($l=6$ or 7). This level is tentatively assigned $\frac{15}{2}^-$[743↑]. The energy and the $(d,p)$ population of this level are very similar to the corresponding values in $^{235}$U. Therefore, the $\frac{7}{2}$[743↑] band head (the ground state in $^{235}$U) is expected close to the ground state in $^{233}$Th. If this $\frac{7}{2}^-$ level had a larger excitation energy than the $\frac{5}{2}^+$[622↑] level, the unsuccessful search for the $\frac{7}{2}^-$ isomer in $^{233}$Th could

be understood.[5,39] The only other member of the [743↑] band which has the possibility of being observed in the $(d,p)$ reaction, the $\frac{11}{2}$ level, seems to be covered by the 106.9-keV level. $\gamma$ transitions to the $\frac{7}{2}$[743↑] level could not be identified by $\gamma$-energy combination, because most of the transitions from higher levels are $K$ forbidden.

The [501↓] configuration has been observed in many actinides.[35,36,48] The level spacing is about 40 keV between the $\frac{1}{2}^-$ and $\frac{3}{2}^-$ level and a few keV between the $\frac{3}{2}^-$ and $\frac{5}{2}^-$ level. The $\frac{1}{2}^-$ and $\frac{3}{2}^-$ levels are supposed to be strongly populated by direct $E1$ transitions. The [501↓] state should appear with low intensity in the $(d,p)$ reaction. The 539.50- and 583.55-keV levels seen in the high-energy $\gamma$-ray spectrum and weakly in the $(d,p)$ reaction are tentatively identified as the $\frac{1}{2}^-$ and $\frac{3}{2}^-$[501↓] states. The $\frac{1}{2}^-$ $(d,p)$ intensity has approximately the correct value, but the $\frac{3}{2}^-$ intensity is too large by more than a factor 5 compared with theoretical values (see Table IV).

This could be caused by an accidental doublet. On the other hand, the $(d,p)$ population of the $\frac{3}{2}^-$ and $\frac{5}{2}^-$ levels in $^{235}$U, both near 703 keV, is as large as the population of the $\frac{1}{2}^-$ level at 659 keV,[35] in contradiction to the theory. Strong admixing with phonon states of the even-even core and Coriolis coupling to the other bands probably explain this serious alternation of the predicted intensity pattern.

### B. Levels Above 500 keV

Many levels above 500 keV have been detected by the $(d,p)$ reaction, by high-energy neutron-capture $\gamma$ rays, and by low-energy $\gamma$-ray combination. Some levels are observed with all three experimental techniques. The identification of these levels is very difficult because of the measured and theoretically expected high level density in this region. The following Nilsson states may be situated above 500 keV: $\frac{1}{2}^+$[620↑], $\frac{1}{2}^-$[761↓], $\frac{3}{2}^+$[622↓], $\frac{3}{2}^-$[761↑], $\frac{3}{2}^-$[501↑], $\frac{5}{2}^-$[752↑], and $\frac{5}{2}^-$[503↓]. In addition to these single-particle configurations one expects $\beta$ and $\gamma$ vibrations coupled to all single-particle states. The theory predicts more than 20 rotational bands between 500 and 1500 keV with the $K$ quantum number less than or equal to $\frac{5}{2}$. The present data are certainly not sufficient to assign configurations to levels in this region unambiguously.

It is interesting to note that the particle states $\frac{1}{2}^+$[620↑], $\frac{3}{2}^+$[622↓], $\frac{7}{2}^+$[613↑], and $\frac{1}{2}^-$[761↓] appear quite indistinct and fragmented in the $^{232}$Th$(d,p)$-$^{233}$Th spectrum. In $(d,p)$ reactions on the even-even uranium, plutonium, and curium isotopes,[29,35,36,49] these same four particle states are strongly excited and easy to recognize. A likely explanation is that for some reason, in $^{233}$Th, phonon excitations of the even-even core strongly admix with these four particle states.

## 4. DISCUSSION

### A. Spectroscopic Factors and Coriolis Mixing

The formulas for the calculation of differential cross sections of the $(d,p)$ reaction and for the extraction of spectroscopic factors $S_{jl}$ including Coriolis mixing have been discussed in several publications[35,50]:

$$\frac{d\sigma}{d\Omega} = N(2j+1)S_{jl}\sigma_{\mathrm{DWBA}},$$

$$S_{jl} = \frac{2}{2j+1}\left(\sum_i a_i C_{jl,i} U_i\right)^2 .$$

The following computational methods and parameters have been used for the calculation of

TABLE V. Rotational bands.

| | Band head (keV) | Fitted band head (keV) | Intrinsic energies (keV) | Single-particle energy Experimental (MeV) | Theoretical without $\epsilon_4$ (MeV) | Theoretical with $\epsilon_4$ (MeV) | Fitted rotational parameter (keV) | $U^2$ assumed |
|---|---|---|---|---|---|---|---|---|
| $\frac{1}{2}$[631↓] | 0 | 0 | −3.23 | +0.346 | +0.346 | +0.346 | 6.47 | 0.76 |
| $\frac{5}{2}$[622↑] | 5.98 | 8.21 | −9.57 | +0.333 | −0.025 | +0.628 | 7.11 | 0.83 |
| $\frac{5}{2}$[633↓] | (262.14) | 262.69 | 247.01 | −0.728 | −0.809 | −0.514 | 6.27 | 0.2 |
| $\frac{7}{2}$[624↓] | 278 | 296.79 | 274.14 | +0.762 | +0.363 | +0.973 | 6.47 | 0.9 |
| $\frac{3}{2}$[631↑] | 335.92 | 335.73 | 326.46 | −0.828 | −1.120 | −0.831 | 6.18 | 0.2 |
| $\frac{7}{2}$[743↑] | (~10) | | (−13) | +0.326 | −0.445 | +0.329 | | 0.76 |
| $\frac{1}{2}$[501↓] | (539.50) | | (536) | −1.076 | −0.368 | −1.618 | | (0.06) |

TABLE VI. Coriolis matrix elements in $^{233}$Th. The experimental values are the fitted matrix elements under the assumption of the reduction factor listed.

| | Experimental value | Reduction factor | Theoretical value without $\epsilon_4$ | Theoretical value with $\epsilon_4$ |
|---|---|---|---|---|
| [631↓]-[631↑] | 0.0097 | 0.7 | −0.077 | −1.01 |
| [622↑]-[631↑] | 4.66 | 0.65 | 4.73 | 5.20 |
| [633↓]-[631↑] | 1.35 | 0.65 | 1.41 | 0.118 |
| [622↑]-[624↓] | 1.03 | 0.40 | 1.17 | −0.232 |
| [633↓]-[624↓] | 4.78 | 0.40 | 4.74 | 4.13 |

$d\sigma/d\Omega$ and $S_{jl}$:

$N = 1.5$: Normalization constant (Ref. 50).

$\sigma_{DWBA}$: Calculated with the program DWUCK[51] by use of optical-model parameters of Ref. 50. $\sigma_{DWBA}$ was computed at excitation energies of 0 and 500 keV and linearly interpolated in between.

$C_{jl}$: Two sets of $C_{jl}$ were used: without $\epsilon_4$ deformation and with $\epsilon_4$ deformation. For the set of $C_{jl}$'s without $\epsilon_4$, the values given by Chi[42] ($\kappa = 0.05$, $\mu = 0.448$ for $N = 6$) with the deformation $\delta = 0.2$ were taken. This deformation was chosen from the table of Löbner, Vetter, and Hönig.[52] The $C_{jl}$'s with $\epsilon_4$ deformation were calculated with a program by Nilsson[43,44] by use of the parameters $\kappa = 0.0635$, $\mu = 0.336$, $\epsilon_2 = 0.2$, and $\epsilon_4 = -0.055$ given in Ref. 43. These $\epsilon_2$ and $\epsilon_4$ are similar to the values measured by Moss *et al.*[53] for $^{232}$Th ($\beta_2 = 0.23$, $\beta_4 = 0.050$).

TABLE VII. $\gamma$ branching ratios.

| Initial state $I_i[Nn_z\lambda\sum]_i$ | Final states $I_f[Nn_z\lambda\sum]_f$ | Experimental | $\gamma$ intensity ratios Calculated with mixing | Calculated without mixing |
|---|---|---|---|---|
| $\frac{7}{2}$[631↑] | $\frac{\frac{7}{2}[631\uparrow]}{\frac{5}{2}[631\downarrow]}$ | $2^{+1.5}_{-1.0}$ | 0.90 | 0.95 |
| $\frac{5}{2}$[631↑] | $\frac{\frac{7}{2}[631\uparrow]}{\frac{5}{2}[631\downarrow]}$ | 0.4 ± 0.1 | 0.2 | 0.2 |
| $\frac{5}{2}$[631↑] | $\frac{\frac{5}{2}[631\uparrow]}{\frac{3}{2}[631\downarrow]}$ | 1.0 ± 0.25 | 0.81 | 0.81 |
| $\frac{5}{2}$[631↑] | $\frac{\frac{3}{2}[631\uparrow]}{\frac{5}{2}[622\uparrow]}$ | $6^{+3}_{-2}$ | 7.0 | 6.8 |
| $\frac{3}{2}$[631↑] | $\frac{\frac{5}{2}[631\uparrow]}{\frac{3}{2}[631\downarrow]}$ | 0.17 ± 0.04 | 0.17 | 0.17 |
| $\frac{3}{2}$[631↑] | $\frac{\frac{3}{2}[631\uparrow]}{\frac{1}{2}[631\downarrow]}$ | 0.83 ± 0.20 | 0.68 | 0.69 |
| $\frac{3}{2}$[631↑] | $\frac{\frac{1}{2}[631\uparrow]}{\frac{5}{2}[622\uparrow]}$ | 4.2 ± 1.0 | 3.1 | 2.8 |
| $\frac{5}{2}$[633↓] | $\frac{\frac{1}{2}[631\uparrow]}{\frac{5}{2}[622\uparrow]}$ | $<2.5 \times 10^{-2}$ | $<10^{-4}$ | $<10^{-4}$ |
| $\frac{5}{2}$[633↓] | $\frac{\frac{7}{2}[622\uparrow]}{\frac{5}{2}[622\uparrow]}$ | 0.19 ± 0.06 | 0.27 | 0.22 |

$U^2$: The pairing emptiness factor is taken from Erskine[54] for the [631↓], [622↑], and [743↑] bands and estimated with a simple pairing calculation[50] for the other bands (see Table V).

Table IV gives experimental and theoretical information on the rotational bands. Columns 1–5 show the excitation energies from the low-energy $\gamma$ rays, the energies from the $(d, p)$ reaction, the calculated energies from the fit to the data including Coriolis mixing (see below), and the $(d, p)$ differential cross section at a laboratory angle of 150°. The experimental cross-section ratio $R_{\text{exp}}$ between 90 and 150° is tabulated in column 6. In the next columns the differential cross sections $\sigma_{\text{DWBA}}(\mu\text{b/sr})$ and the ratio $R_{\text{theor}} = d\sigma(90°)/d\sigma(150°)$ calculated with the distorted-wave Born-approximation (DWBA) code are shown. The experimental spectroscopic factors $S_{jl,\text{exp}}$ are derived from the measured differential cross section at 150° with the formula

$$S_{jl,\text{exp}} = \frac{(d\sigma/d\Omega)_{150°}}{N(2j+1)\sigma_{\text{DWBA}}} .$$

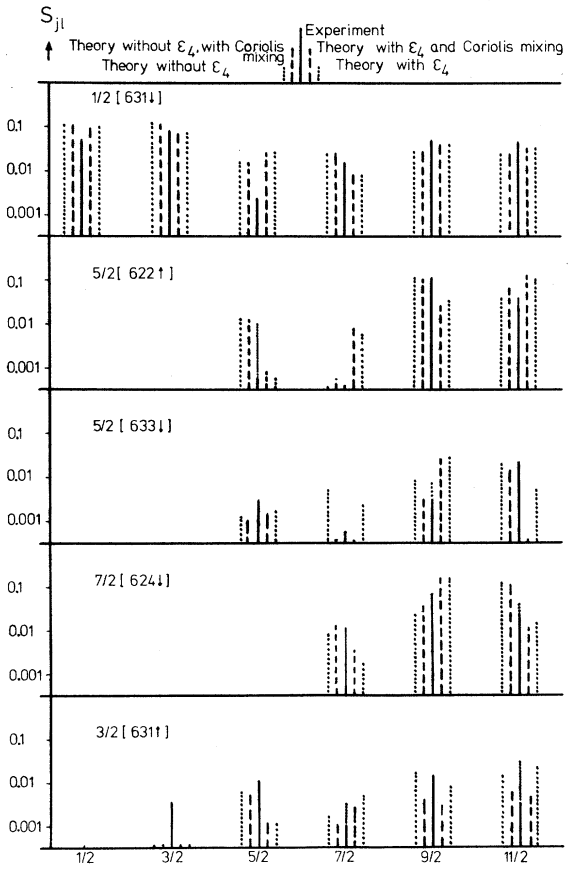


FIG. 6. Experimental and theoretical spectroscopic factors.

The theoretical spectroscopic factors $S_{jl}$ have been calculated without Coriolis mixing for both sets of $C_{jl}$ with $S_{jl} = [2/(2j+1)]C_{jl}^2 U^2$. A fit to the experimental energies has been performed with the computer program BANDFIT[55] for the five positive-parity bands at low energy. Coriolis band mixing is included by the program. Five moments of inertia, four band-head energies, one decoupling parameter, and five Coriolis matrix elements $\langle K|j_-|K+1\rangle$ have been searched to fit 19 level energies [0, 6.0, 16.9, 50.3, 54.6, 93.7, 106.9, 159.0, 178, 220, 262.1, 278, 326.0, 335.9, 371.2, 388.5 (2 times), 464, 480.9, all in keV]. $\Delta E_{\text{rms}}$, the average deviation, is 1.6 keV. This good agreement is strong supporting evidence for the assignment of the five rotational bands. The fitted band-head energies (of the unperturbed bands) and the fitted rotational parameters $A = \hbar^2/2\mathcal{I}$ are listed in Table V.

The fitted Coriolis matrix elements are compared with theoretical values (for formulas see Ref. 50) in Table VI. During the fitting calculation, a further reduction of the matrix elements was applied through the use of the empirical reduction factors found by Casten *et al.*[56] Fits could not be achieved without these reduction factors. The agreement of the experimental matrix elements and the theoretical ones without $\epsilon_4$ is excellent. The fitted level energies are given in Table IV.

The spectroscopic factors $S_{jl}$ including Coriolis mixing are also listed in Table IV. Figure 6 illustrates for all five bands the relations between

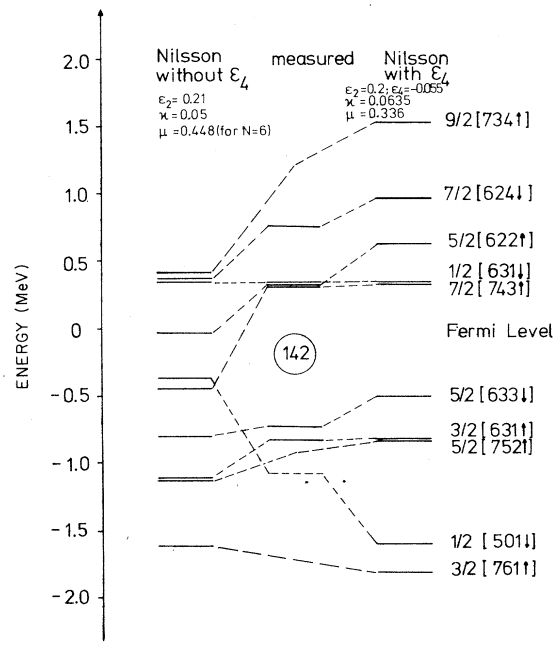


FIG. 7. Single-particle energies in $^{233}$Th.

the experimental and different theoretical spectroscopic factors. There is reasonable agreement between the experimental $S_{jl}$ and the $S_{jl}$ calculated without $\epsilon_4$ and with Coriolis mixing in most cases. For the [622↑] and [631↑] bands the $S_{jl}$ without $\epsilon_4$ and without Coriolis mixing tend to give better agreement. Large discrepancies between $S_{jl}$ with Coriolis mixing and with $\epsilon_4$ and $S_{jl,\mathrm{exp}}$ show up in the following states: $\frac{9}{2}$[622↑], a factor 4 too small; $\frac{11}{2}$[622↑], a factor 5 too large; $\frac{9}{2}$[633↓], a factor >3 too large; $\frac{11}{2}$[633↓], a factor >20 too small; $\frac{7}{2}$[624↓], a factor 3 too small; $\frac{5}{2}$[631↑], a factor 10 too small; $\frac{9}{2}$[631↑], a factor 5 too small. Examination of Fig. 6 shows that the wave functions including $\epsilon_4$ calculated with the program of Ref. 44 do not fit the experimental $(d,p)$ intensities quite as well as the wave functions without $\epsilon_4$.

### B. γ Branching Ratios

With the mixing amplitudes from the five-band Coriolis-coupling calculation we determined the $E2$ and $M1$ transition probabilities and branching ratios between these bands. The $E2$ transitions were calculated under the simplifying assumption of a common quadrupole momentum for all bands $Q_0 = 9\ e$ b. In addition, the $E2$ transition probability between Nilsson states was neglected compared with the much greater collective $E2$ strength. For the $M1$ transitions the undisturbed $M1$ matrix elements were obtained from the $C_{jl}$'s of the $\epsilon_4$ Nilsson calculation. However, it was necessary to reduce the matrix element between the [631↑] and the [622↑] states by a factor 3 to explain the transitions between these two bands. These transitions are very little influenced by Coriolis coupling. The formulas used for the calculation of the transition probabilities are given by Brockmeier *et al.*[57]

Table VII, in which the calculated branching ratios are compared with the experimental results, shows good agreement in all cases. At the same time one sees the negligible influence of the coupling on these transitions. This fact is expected, since the states [631↓], [631↑], and [622↑] do not mix very much.

### C. Single-Particle Energies

The computer programs which were used for the calculation of the $C_{jl}$'s[42-44] also yield the single-particle energies listed in Table V (with and without $\epsilon_4$ deformation). All these calculations were performed with the parameters given in Sec. 4 A. The single-particle energies have been adjusted to the ground-state ($K = \frac{1}{2}$) value of $(\epsilon_{1/2} - \lambda) = 0.346$ MeV. This figure was obtained from even-odd atomic mass differences[27] $\{M(^{233}\mathrm{Th}) - \frac{1}{2}[M(^{232}\mathrm{Th}) + M(^{234}\mathrm{Th})] = 0.696\ \mathrm{MeV}\}$ with the use of $\Delta = 0.6$ MeV[54] and the simple equation for the intrinsic energies,[50] $E^K_{\mathrm{intr.}} = [(\epsilon_K - \lambda)^2 + \Delta^2]^{1/2} - 0.696$ MeV.

The intrinsic energies ($E^K_{\mathrm{intr.}}$) listed in Table V were derived from the fitted band-head energies by subtraction of $AK$ by use of the formula $E^K_I = E^K_{\mathrm{intr.}} + A[I(I+1) - K^2]$. For the calculation of experimental single-particle energies $(\epsilon_K - \lambda)$, the simple pairing formalism[50] has been applied, although it should be emphasized that the uncertainty of the procedure is larger in the present case than usual, because in $^{233}$Th the single-particle energies are not equally distributed and there is a gap close to the ground state.

The experimental and theoretical single-particle energies are compared in Table V and Fig. 7. The theoretical values including $\epsilon_4$ reproduce better the experimental values than the ones without $\epsilon_4$. The experimental energies lie in between the two theoretical energies. For comparison it is interesting to see how level energies are shifted if two protons or two neutrons are added to a nucleus. This shift of experimental band-head energies in the thorium isotopes and in the 143-neutron isotones is demonstrated in Fig. 8. The level scheme of $^{237}$Pu is taken from private communications,[46,47] the $^{235}$U scheme from Braid *et al.*,[35]

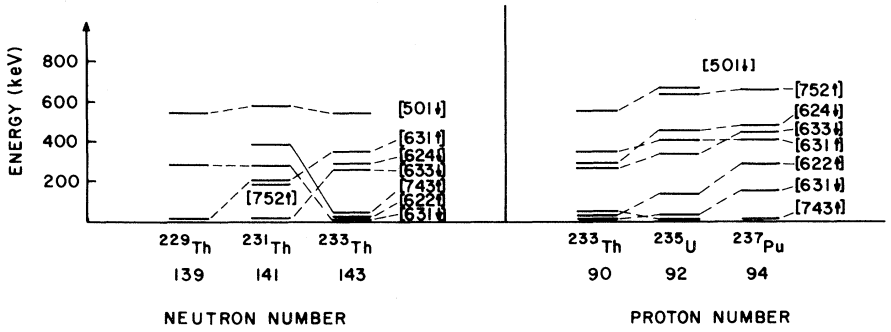


FIG. 8. Band-head energies in the Th isotopes and 143-neutron isotones.

the $^{231}$Th scheme from Elze, von Egidy, and Huizenga,[58,59] and the $^{229}$Th scheme from Braid *et al.*[60] The figure of the isotones shows that all levels seem to be lowered if two protons are removed from the nucleus. This compression might be caused by the stronger influence of quadrupole and octupole vibrations.


## ACKNOWLEDGMENTS

We wish to thank I. Hamamoto, H. J. Mang, L. A. Malov, and K. Nybö for valuable discussions, M. Waldschmidt for measuring the reaction $^{232}$Th-$(n, e)^{233}$Th, and W. Kallinger for evaluating some $(n, \gamma)$ data.


---

*Work supported in part by the U. S. Atomic Energy Commission.

† Present address: Tata Institute of Fundamental Research, Bombay, India.

‡ Present address: Institut Max v. Laue-Paul Langevin, Grenoble, France.


[1]N. A. Burgow and J. V. Danilian, Izv. Akad. Nauk. SSSR, Ser. Fiz. 20, 941 (1956) [transl.: Bull. Acad. Sci. USSR, Phys. Ser. 20, 852 (1956)].

[2]L. V. Groshev, A. M. Demidov, V. N. Lutsenko, and V. I. Pelekhov, *Atlas of Gamma-Ray Spectra from Radiative Capture of Thermal Neutrons* (Pergamon, London, 1959).

[3]R. C. Greenwood and J. H. Reed, IIT Research Institute, Chicago, Ill., Report No. IITRI-1193-53, 1965 (unpublished), Vol. 1.

[4]K. Kernbach, N. F. Fiebiger, and K. Stelzer, KFA Jülich, Germany, Report No. Jül-Conf-1, 1967 (unpublished), p. 50.

[5]W. Hoekstra, Ph.D. thesis, Technische Hogeschool, Delft, The Netherlands, 1969 (unpublished).

[6]J. Kern, Fribourg, Switzerland, private communication.

[7]T. Grotdal, J. Limstrand, K. Nybö, K. Skår, and T. F. Thorsteinsen, University of Bergen, Norway (unpublished).

[8]O. A. Wasson, J. B. Garg, R. E. Chrien, and M. R. Bhat, *Neutron Cross Sections and Technology* (National Bureau of Standards, Washington, D. C., 1968), Vol. II, p. 675.

[9]T. von Egidy, O. W. B. Schult, D. Rabenstein, R. E. Chrien, J. R. Erskine, H. A. Baader, and D. Breitig, Verhandl. Deut. Physik. Ges. 6, 248 (1971).

[10]T. von Egidy, in *Neutron Capture Gamma-Ray Spectroscopy* (International Atomic Energy Agency, Vienna, Austria, 1969), p. 127.

[11]M. Waldschmidt and P. Osterman, Z. Physik 247, 153 (1971).

[12]H. R. Koch, H. A. Baader, D. Breitig, K. Mühlbauer, U. Gruber, B. P. K. Maier, and O. W. B. Schult, in *Neutron Capture Gamma-Ray Spectroscopy* (see Ref. 10), p. 65.

[13]E. R. Cohen and J. W. M. DuMond, Rev. Mod. Phys. 37, 537 (1965).

[14]S. Hagström, C. Nordling, and K. Siegbahn, in *Alpha-, Beta-, and Gamma-Ray Spectroscopy*, edited by K. Siegbahn (North-Holland, Amsterdam, 1965), p. 845.

[15]R. G. Albridge, J. M. Hollander, C. J. Gallagher, and J. H. Hamilton, Nucl. Phys. 27, 529 (1961).

[16]T. von Egidy, O. W. B. Schult, W. Kallinger, D. Breitig, R. P. Sharma, H. R. Koch, and H. A. Baader, Z. Naturforsch. 26a, 1092 (1971).

[17]D. Rabenstein, Ph.D. thesis, Technical University Munich, 1970 (unpublished).

[18]T. von Egidy, K. Böning, H. Heidemann, L. Koester, and D. Rabenstein, in *Research Reactor Utilization* (International Atomic Energy Agency, Vienna, Austria, 1970), Vol. I, p. 225.

[19]R. C. Greenwood and W. W. Black, Phys. Letters 21, 702 (1966).

[20]R. E. Chrien and M. Reich, Nucl. Instr. Methods 53, 93 (1967).

[21]G. Murray, R. L. Graham, and J. S. Geiger, Nucl. Phys. 63, 353 (1965).

[22]W. R. Kane, Brookhaven National Laboratory, private communication.

[23]L. V. Groshev, A. M. Demidov, V. A. Ivanov, N. N. Lutsenko, and V. I. Pelekhov, Izv. Akad. Nauk. SSSR, Ser. Fiz. 27, 1377 (1963) [transl.: Bull. Acad. Sci. USSR, Phys. Ser. 27, 1353 (1963)].

[24]M. R. Bhat and R. E. Chrien, Phys. Rev. 155, 1362 (1967).

[25]R. E. Wood, Phys. Rev. 98, 639 (1955).

[26]C. E. Porter and R. G. Thomas, Phys. Rev. 104, 483 (1956).

[27]H. A. Wapstra and N. B. Gove, Nucl. Data A9, 265 (1971).

[28]E. T. Jurney, in *Neutron Capture Gamma-Ray Spectroscopy* (see Ref. 10), p. 431.

[29]R. K. Sheline, W. N. Shelton, T. Udagawa, E. T. Jurney, and H. T. Motz, Phys. Rev. 151, 1011 (1966).

[30]D. L. Price, R. E. Chrien, O. A. Wasson, M. R. Bhat, M. Boer, M. A. Lone, and R. Graves, Nucl. Phys. A121, 630 (1968).

[31]L. M. Bollinger and G. E. Thomas, Phys. Rev. C 2, 1951 (1970).

[32]J. E. Spencer and H. A. Enge, Nucl. Instr. Methods 49, 181 (1967).

[33]J. R. Erskine and R. H. Vonderohe, Nucl. Instr. Methods 81, 221 (1970).

[34]P. Spink and J. R. Erskine, Argonne National Laboratory, Physics Division Informal Report No. PHY-1965 B (unpublished); and J. R. Comfort, Argonne National Laboratory, Physics Division Informal Report No. PHY-1970 B (unpublished).

[35]T. H. Braid, R. R. Chasman, J. R. Erskine, and A. M. Friedman, Phys. Rev. C 1, 275 (1970).

[36]T. H. Braid, R. R. Chasman, J. R. Erskine, and A. M. Friedman, Phys. Rev. C 4, 247 (1971).

[37]N. Williams, private communication.

[38]J. E. Cline, Nucl. Phys. A106, 481 (1968).

[39]W. Hoekstra and A. H. Wapstra, Phys. Rev. Letters 22, 859 (1969).

[40]C. Sebille, G. Bastin, C. F. Leang, and R. Piepen-

bring, C. R. Acad. Sci. Paris 270, 354 (1970).
[41]We wish to acknowledge the helpful discussions on the decay of $^{233}$Th with Dr. Claire Sebille.
[42]B. E. Chi, Nucl. Phys. 83, 97 (1966); and State University of New York at Albany Report, 1967 (unpublished).
[43]S. G. Nilsson, C. F. Tsang, A. Sobiczewski, Z. Szymanski, S. Wycech, C. Gustavson, I.-L. Lamm, P. Möller, and B. Nilsson, Nucl. Phys. A131, 1 (1969).
[44]B. Nilsson, $\epsilon_4$ Program, Program Library, Nordita, Copenhagen, (unpublished).
[45]L. A. Malov and V. G. Soloviev, Yadern. Fiz. 5, 566 (1967) [transl.: Soviet J. Nucl. Phys. 5, 403 (1967)].
[46]I. Ahmad, Argonne National Laboratory, private communication.
[47]K. Nybö, University of Bergen, Norway, private communication.
[48]T. von Egidy, Th. W. Elze, and J. R. Huizenga, Nucl. Phys. A145, 306 (1970).
[49]T. H. Braid, R. R. Chasman, J. R. Erskine, and A. M. Friedman, Phys. Letters 18, 149 (1965).
[50]B. Elbeck and P. O. Tjöm, in *Advances in Nuclear Physics*, edited by M. Baranger and E. Vogt (Plenum, New York, 1969), Vol. 3, p. 259.
[51]We are indebted to R. Santo and G. Gaul for providing the DWBA calculations.
[52]K. E. G. Löbner, M. Vetter, and V. Hönig, Nucl. Data A7, 495 (1970).
[53]J. M. Moss, Y. D. Terrien, R. M. Lombard, C. Brassard, J. M. Loiseaux, and F. Resmini, Phys. Rev. Letters 26, 1488 (1971).
[54]J. R. Erskine, Phys. Rev. C 5, 959 (1972).
[55]This code was developed by E. Sutter and J. R. Erskine.
[56]R. F. Casten, P. Kleinheinz, P. J. Daly, and B. Elbek, Phys. Rev. C 3, 1271 (1971).
[57]R. T. Brockmeier, S. Wahlborn, E. J. Seppi, and F. Boehm, Nucl. Phys. 63, 102 (1965).
[58]Th. W. Elze, T. von Egidy, and J. R. Huizenga, Nucl. Phys. A128, 564 (1969).
[59]J. S. Boyno, Th. W. Elze, and J. R. Huizenga, Nucl. Phys. A154, 263 (1970).
[60]T. H. Braid, R. R. Chasman, J. R. Erskine, and A. M. Friedman, unpublished.

PHYSICAL REVIEW C VOLUME 6, NUMBER 1 JULY 1972

# Compound Spreading Widths for $Bi^{209}$ Analog Resonances*

William P. Beres and David A. Voges
*Department of Physics, Wayne State University, Detroit, Michigan 48202*
(Received 7 January 1972)

The compound spreading widths (due to the Coulomb interaction) of $\frac{9}{2}^+$, $\frac{11}{2}^+$, $\frac{15}{2}^-$, $\frac{1}{2}^+$, $\frac{7}{2}^+$, and $\frac{3}{2}^+$ analog resonances in $Bi^{209}$ are calculated within the general framework of the de Toledo Piza–Kerman scheme by relegating the giant isovector monopole contributions to the continuum space. The work emphasizes the structure of the parent states and the coupling is via $[H_c, T_-]$. The widths are found to be of the order of 20 keV, which is considerably less than the observed experimental total widths of 200–300 keV. A background of (i) configuration states (6 including the antianalog state for each analog resonance) and (ii) complex levels (e.g., 33 261 states for $\frac{9}{2}^+$ are considered. The one-body Coulomb interaction represented by a uniform sphere of charge is used for (i), while the two-body Coulomb force is expanded in multipoles for (ii). In (i) the dependence on the Coulomb radius and the nuclear spreading width are also studied. For all doorways the relative importance, number, density, strength, and compound-width contributions are investigated in great detail and the results are presented in tables and histograms. In addition to certain states of type (i) the most significant complex states are those based on the $Pb^{208}$ giant dipole doorway resonance.

## I. INTRODUCTION

The discovery of isobaric analog resonances as members of isobaric multiplets has led to much experimental and theoretical activity.[1] If, e.g., an analog resonance is formed by proton bombardment of a target nucleus $(Z, N)$ with isospin quantum numbers $(T, T)$, then the analog resonance is in the nucleus $(Z+1, N)$, and the quantum numbers are $(T+\frac{1}{2}, T-\frac{1}{2})$. This state is considered to be the second member of a $2T+2$ multiplet, the first member of which is the parent state $(T+\frac{1}{2}, T+\frac{1}{2})$. This level is a low-lying bound state in the adjacent parent nucleus $(Z, N+1)$. Isospin-violating forces (primarily the Coulomb repulsion among protons) remove the energy degeneracy of the multiplet members and shift the analog state upward into the continuum. In addition to this gross shift the isospin of the analog level ceases to be pure. The long-range Coulomb force results, however, in only weak coupling to the vast horde of neighboring states of lower isospin $(T-\frac{1}{2}, T-\frac{1}{2})$. We will